AD_____

Award Number: W81XWH-05-1-0390

TITLE: Chemoprevention of Breast Cancer by Mimicking the Protective Effect of Early First Birth

PRINCIPAL INVESTIGATOR: Malcolm C. Pike, Ph.D.

CONTRACTING ORGANIZATION: University of Southern California
Los Angeles, CA 90089-1147

REPORT DATE: June 2008

TYPE OF REPORT: Annual

PREPARED FOR: U.S. Army Medical Research and Materiel Command
Fort Detrick, Maryland 21702-5012

REPORT DOCUMENTATION PAGE

Form Approved
OMB No. 0704-0188

1. REPORT DATE *(DD-MM-YYYY)*	**2. REPORT TYPE**	**3. DATES COVERED** *(From - To)*
01-06-2008	Annual	2 May 2007 – 2 May 2008

4. TITLE AND SUBTITLE

Chemoprevention of Breast Cancer by Mimicking the Protective Effect of Early First Birth

5a. CONTRACT NUMBER

5b. GRANT NUMBER
W81XWH-05-1-0390

5c. PROGRAM ELEMENT NUMBER

6. AUTHOR(S)

Malcolm C. Pike, Ph.D.

E-Mail: mcpike@usc.edu

5d. PROJECT NUMBER

5e. TASK NUMBER

5f. WORK UNIT NUMBER

7. PERFORMING ORGANIZATION NAME(S) AND ADDRESS(ES)

University of Southern California
Los Angeles, CA 90089-1147

8. PERFORMING ORGANIZATION REPORT NUMBER

9. SPONSORING / MONITORING AGENCY NAME(S) AND ADDRESS(ES)
U.S. Army Medical Research and Materiel Command
Fort Detrick, Maryland 21702-5012

10. SPONSOR/MONITOR'S ACRONYM(S)

11. SPONSOR/MONITOR'S REPORT NUMBER(S)

12. DISTRIBUTION / AVAILABILITY STATEMENT
Approved for Public Release; Distribution Unlimited

13. SUPPLEMENTARY NOTES – Original contains colored plates: ALL DTIC reproductions will be in black and white.

14. ABSTRACT

We have successfully shown that in the rat estradiol, estradiol plus progesterone, and beta-HCG is protective against carcinogen-induced mammary tumorigenesis. Progesterone alone was not protective; perphenazine was partially protective. Treatment and pregnancy induced RNA gene expression changes have been identified. Work on finding the lowest effective dose of estrogen has started. We have continued to collect normal breast tissue from women undergoing elective reduction mammoplasty. Estrogen receptor, progesterone receptors and cell proliferation have been characterized and compared to breast tissue obtained from women in the first trimester of pregnancy. RNA characterization of these samples has begun. Two chemoprevention protocols have been developed. The first evaluates the role of high dose progestins on cell proliferation and gene expression profiles in the breast; recruitment is ongoing. The second evaluates the role of various oral contraceptive progestin doses on cell proliferation and gene expression profiles in the breast; recruitment will be complete by the end of October 2008. Pregnancy reduces mammographic density and breast cancer risk. How these are related has been studied in a large autopsy series; results suggest that part of the protection may be the result of a reduction in breast epithelium.

15. SUBJECT TERMS
No subject terms

16. SECURITY CLASSIFICATION OF:			**17. LIMITATION OF ABSTRACT**	**18. NUMBER OF PAGES**	**19a. NAME OF RESPONSIBLE PERSON**
a. REPORT	**b. ABSTRACT**	**c. THIS PAGE**			USAMRMC
U	U	U	UU	64	**19b. TELEPHONE NUMBER** *(include area code)*

Table of Contents

INTRODUCTION: This Innovator Award is designed to provide insight into the ways in which a chemoprevention regimen can mimic the protective effect of a full-term pregnancy (a birth) against breast cancer. In addition, we are aiming to understand the mechanisms underlying the risk associated with increased mammographic density, the strongest known risk factor for breast cancer after the highly penetrant genetic risk factors of BRCA1 and BRCA2 mutations. Mammographic densities are permanently reduced by births; and this relationship is being explored in depth in order to determine if this is an important part of the mechanism by which births provide protection against breast cancer. This work is being conducted both in humans and rodents.

BODY: The Innovator Award consists of four projects (Projects 1 and 2 are being completed through a subcontract to our colleague Dr. Lewis Chodosh at the University of Pennsylvania, and Projects 3 and 4 are being completed by the team at USC).

Task 1: Months 1-12: Treat rats with different hormonal chemoprevention regimens, harvest mammary tissue, and isolate RNA.

This task has been completed on schedule. Groups of Lewis rats have been treated with pellets containing either estradiol, progesterone, estradiol and progesterone, beta-HCG, or perphenazine. Animals were treated for 21 days. Pellets were then removed and animals sacrificed 28 days later. Control groups consisted of parous animals allowed to undergo a single round of pregnancy, lactation, and 28 days of involution, as well as age-matched nulliparous controls. For all groups, total RNA was prepared from mammary glands by ultracentrifugation through a CsCl/guanidinium isothiocyanate cushion.

The effects of each of these hormonal treatments on the susceptibility to MNU-induced mammary tumorigenesis was tested using standard protocols either with MNU administered before hormonal treatments or after. Similar results were obtained and confirmed that treatment with estradiol, estradiol and progesterone, or beta-HCG is protective against mammary tumorigenesis, whereas treatment with progesterone is not. Additionally, we found that treatment with perphenazine was partially protective against MNU-induced tumorigenesis.

Task 2: Months 6-24: Analyze morphological changes and determine global gene expression profiles for rat mammary gland samples from rats treated with different hormonal chemoprevention regimens.

This task has been completed on schedule. Analysis of mammary gland morphology by carmine stained whole mounts as well as by hematoxylin and eosin-stained sections indicated that after 21 days of hormone treatment, estradiol, estradiol and progesterone, beta-HCG, and perphenazine each gave rise to mammary epithelial differentiation comparable to that observed in mid-pregnant animals. In contrast, treatment with progesterone had no effect on mammary epithelial morphology.

Mammary gland morphology was also examined following 28 days of involution following treatment termination. This analysis revealed that mammary gland morphology was extremely similar among all groups and that there were not obvious differences in the amount of epithelium present.

RNA prepared from each of these experimental groups was used to generate biotinylated cRNA suitable for hybridization to Affymetrix oligonucleotide microarrays. Each of these samples was subsequently hybridized to Affymetrix microarrays. Array results have been analyzed and quality control parameters have confirmed successful hybridization and scanning of the arrays. Analyses of these microarray data sets have also been performed to identify genes that are differentially expressed as a consequence of each hormonal treatment regimen.

All hormone treatments, in addition to pregnancy, led to significant gene expression changes in the mammary gland after 4 weeks of regression (Table 1). The number of differentially expressed genes in response to pregnancy and progesterone treatment was relatively small, while estradiol, estradiol plus progesterone, HCG, and perphenazine treatment led to more widespread gene expression changes.

Experimental condition	Baseline condition	Differentially Expressed Genes (Experimental/Baseline)		
		Total	Up-regulated	Down-regulated
G1P1	G0P0	314	137	177
P	G0P0	294	132	162
E	G0P0	1613	905	708
E+P	G0P0	1559	655	904
HCG	G0P0	1206	443	763
PPZ	G0P0	1431	565	866

Table 1. Differentially expressed genes in response to various hormone treatments. Rats were treated with the indicated hormones for 21 days, and the mammary gland was allowed to regress for 28 days following treatment termination. Genes differentially expressed in response to each treatment compared to nulliparous controls (G0P0) were identified by microarray analysis. Differentially expressed genes were identified by CyberT at an FDR <10%.

We next sought to identify genes that are differentially expressed in response to protective, but not non-protective, hormonal treatments. Perphenazine treatment conferred only partial protection against MNU-induced tumorigenesis and elicited variable degrees of mammary epithelial differentiation. To avoid confounding effects of this heterogeneity, we excluded perphenazine-treated rats from this analysis. We compared genes commonly up- or down-regulated by protective (G1P1, E, E+P, and HCG) but not non-protective (P) regimens. This analysis identified 47 genes commonly upregulated (Table 2) and 28 genes commonly downregulated (Table 3) in protective hormone treatments, but that were unaltered in non-protective treatments. These represent promising candidates for genes that are responsible for the chemopreventive effects of these hormonal regimens.

Gene ID	Symbol	Name
29173	Csn2	casein beta
114595	Csng	casein gamma
114596	Wap	whey acidic protein
314487		Partial mRNA for immunoglobulin alpha heavy chain (partial), complete constant region
394266	Gjb2	gap junction membrane channel protein beta 2
54231	Ca2	carbonic anhydrase 2
29229	Spt1	salivary protein 1
117033	Mmp12	matrix metalloproteinase 12
24903	Kng	T-kininogen
24284	Csn1	Casein, alpha
Gene ID	**Symbol**	**Name**
54231	Ca2	carbonic anhydrase 2
24567	Mt1a	Metallothionein
29469	Lbp	lipopolysaccharide binding protein
24528	Lalba	lactalbumin, alpha
24567	Mt1a	Metallothionein
64669	Mch	medium-chain S-acyl fatty acid synthetase thio ester hydrolase (MCH)
24567	Mt1a	Metallothionein
170496	Lcn2	lipocalin 2
79131	Fabp3	fatty acid binding protein 3
29188	Csn10	casein kappa
171578	Muc4	mucin 4
24571	Muc1	mucin 1
24191	Aldoc	aldolase C, fructose-biphosphate
25046	Pigr	polymeric immunoglobulin receptor
24191	Aldoc	aldolase C, fructose-biphosphate
81503	Gro1	gro
24825	Tf	Transferrin
361725	MGC72333	similar to PROSTATIC STEROID-BINDING PROTEIN C3 CHAIN PRECURSOR (PROSTATEIN PEPTIDE C3)
25717	Tgfb3	transforming growth factor, beta 3
24825	Tf	Transferrin
83497	Ocln	occludin
25145	Cd24	CD24 antigen
83497	Ocln	occludin
29285	Rps15	ribosomal protein S15
362350		Rat T-cell receptor active beta-chain C-region mRNA, partial cds, clone TRB4
25277	Mfge8	milk fat globule-EGF factor 8 protein
60350	Cd14	CD14 antigen
25717	Tgfb3	transforming growth factor, beta 3
24268	Cp	ceruloplasmin
25055	Lipa	lipase A, lysosomal acid
294257	Bf	B-factor, properdin
60350	Cd14	CD14 antigen
25275	Cnp1	cyclic nucleotide phosphodiesterase 1
298199	ADRP	adipose differentiation-related protein
24767	Scnn1b	sodium channel, nonvoltage-gated 1 beta
54410	LOC54410	alkaline phosphodiesterase
25279	Cyp24	cytochrome P450, subfamily 24

Table 2. Genes commonly and uniquely upregulated in response to protective hormonal regimens (E, E+P, HCG) or parity compared to nulliparous rats.

Gene ID	Symbol	Name
50561	Resp18	regulated endocrine-specific protein 18
25492	Nfia	nuclear factor I/A
94339	Mmp23	Matrix metalloproteinase 23
50658	Mapk9	stress activated protein kinase alpha II
Gene ID	**Symbol**	**Name**
81008	Itga7	integrin alpha 7
29637	Hmgcs1	3-hydroxy-3-methylglutaryl-Coenzyme A synthase 1
60627	LOC60627	component of rsec6/8 secretory complex p71 (71 kDa)
140808	Enman	endo-alpha-mannosidase
25157	Plagl1	pleiomorphic adenoma gene-like 1
24472	Hspa1a	heat shock 70kD protein 1A
64030	Kit	c-kit receptor tyrosine kinase
65028	Hsj2	DnaJ-like protein
83626	Ugcg	UDP-glucose:ceramide glycosyltransferase
29650	Adam10	a disintegrin and metalloprotease domain 10
309798		Similar to Golgi coiled coil protein GCC185 (LOC309798), mRNA
64831	Ireb2	iron-regulatory protein 2
24848	Tph	tryptophan hydroxylase
25230	Add3	adducin 3, gamma
117255	Ptpn12	protein tyrosine phosphatase, non-receptor type 12
29416	Kat2	kynurenine aminotransferase 2
25382	Aplp2	amyloid beta (A4) precursor-like protein 2
24553	Met	met proto-oncogene
25510	Pcp4	Purkinje cell protein 4
54245	Crko	avian sarcoma virus CT10 (v-crk) oncogene homolog
24679	Prkar2b	protein kinase, cAMP dependent regulatory, type II beta
25404	Cav	caveolin
79124	Anxa4	ZAP 36/annexin IV
25705	Tcf8	transcription factor 8

Table 3. Genes commonly and uniquely downregulated in response to protective hormonal regimens (E, E+P, HCG) or parity compared to nulliparous rats.

Task 3: Months 6-36: Identify genes that are expressed in a parity-specific manner in the rat.

This task has been completed ahead of schedule and was published in *Cancer Research* (Blakely et al., 66:6421-6431, 2006; erratum in 67:844-846), where it was featured on the cover.

A major challenge posed by global gene expression surveys is the large number of differentially expressed genes that are typically identified, only a few of which may contribute causally to the phenomenon under study. Consequently, we considered approaches to identifying parity-induced changes in the rat mammary gland that would permit the resulting list of expressed genes to be narrowed to those most robustly associated with parity-induced protection against mammary tumorigenesis. Given the marked genetic and biological heterogeneity between different inbred rat strains, we reasoned that identifying expression changes that are conserved across multiple strains exhibiting hormone-induced protection against mammary tumorigenesis would facilitate the identification of a core set of genes associated with parity-induced protection against breast cancer.

To achieve this goal, we focused on gene expression changes that are conserved among different strains of rats that exhibit hormone-induced protection against mammary tumorigenesis. Four inbred rat strains that exhibit marked differences in their intrinsic susceptibilities to carcinogen-induced mammary tumorigenesis were each demonstrated to display significant protection against MNU-induced mammary tumorigenesis following treatment with pregnancy levels of estradiol and progesterone. Microarray expression profiling of parous and nulliparous mammary tissue from these four strains yielded a common 70-gene signature. Examination of the genes constituting this signature implicated alterations in TGF-beta signaling, the extracellular matrix, amphiregulin expression, and the growth hormone-Igf1 axis in pregnancy-induced alterations in breast cancer risk. Notably, related changes have been associated with decreased mammographic density, which itself is strongly associated with decreased breast cancer risk. Our findings demonstrate that hormone-induced protection against mammary tumorigenesis is widely conserved among divergent rat strains and define a gene expression signature that is tightly correlated with reduced mammary tumor susceptibility as a consequence of a normal developmental event. Given the conservation of this signature, these pathways may contribute to pregnancy-induced protection against breast cancer.

Task 4: Months 6-36: Identify genes whose expression in rats correlates with protection against breast cancer.

This task has been completed ahead of schedule. To narrow the list of candidate genes whose regulation might contribute to the protected state associated with parity, we attempted to identify parity-induced gene expression changes that correlated with protection across multiple rat strains. To this end, total RNA was isolated from the mammary glands of nulliparous and parous Wistar-Furth, Fischer 344, and Copenhagen rats and analyzed on RGU34A arrays. This led to the identification of 68, 64 and 92 parity-up-regulated genes and 132, 209 and 149 parity-down-regulated genes in Wistar-Furth, Fischer 344, and Copenhagen rats, respectively.

Unsupervised hierarchical clustering performed using the expression profiles of 1,954 globally varying genes across the nulliparous and parous datasets representing the four rat strains revealed that samples clustered primarily based on strain without regard to parity status. This suggested that the principal source of global variation in gene expression across these data sets was due to genetic differences between strains rather to than reproductive history. This observation suggested that determining which parity-induced gene expression changes were conserved among these highly divergent rat strains could represent a powerful approach to defining a parity-related gene expression signature correlated with hormone-induced protection against mammary tumorigenesis.

To identify parity-induced gene expression changes that were conserved across strains, we selected genes that exhibited $\geq$ 1.2-fold change in at least of 3 of the 4 strains analyzed. This led to the identification of 24 up-regulated and 46 down-regulated genes. Based on the number of parity-induced gene expression changes observed for each strain, an overlap of this size is highly unlikely by chance (up-regulated: $P<1x10^{-6}$, FDR < 1%; down-regulated: $P<1x10^{-6}$, FDR = 4%). As such, this approach led to the identification of a set of genes whose expression is persistently altered by parity across multiple strains of rats that exhibit hormone-induced protection against mammary tumorigenesis.

To confirm the validity of the parity-related gene expression signature derived

from the above studies, we performed oligonucleotide microarray analysis on samples from nulliparous and parous Lewis rats that were generated independently from those used to derive this signature. Hierarchical clustering analysis of these independent samples using the gene signature revealed that the expression profiles of these genes were sufficient to accurately distinguish parous from nulliparous Lewis rat samples in a blinded manner.

To determine whether this parity-related signature could distinguish between nulliparous and parous mammary glands from multiple strains of rats, Lewis, Wistar-Furth, Fischer 344, and Copenhagen microarray data sets were clustered in an unsupervised manner based solely on the expression of the genes comprising the parity signature. In each of the four rat strains examined, the gene expression signature was sufficient to distinguish parous from nulliparous rats. Thus, this signature reflects parity-induced gene expression changes that are highly conserved among four genetically divergent rat strains.

Among the genes that we identified as being consistently regulated by parity, at least five categories were evident. These included the previously identified differentiation, immune, Tgf-beta, and growth factor categories, as well as an additional category of genes that are involved in extracellular matrix (ECM) structure and function. We next demonstrated that clustering based upon genes in each of these five categories was sufficient to distinguish between nulliparous and parous mammary samples from each of the four different rat strains, from independent mammary samples derived from nulliparous and parous Lewis rats, and from mammary samples derived from FVB mice. These findings indicate that differential expression of these five subsets of genes represent conserved features of parity-induced changes in the rodent mammary gland. Our findings have now been published in *Cancer Research* (Blakely *et al*., 66:6421-6431, 2006; erratum in 67:844-846).

Task 5: Months 1-48: Isolate RNA from human mammary gland samples and control epithelial and stromal samples.

Per the SOW, significant progress has been made on this aim. RNA has been isolated from a large number of the available human specimens. In addition, we have prepared RNA from control samples consisting of: intact adipose tissue, intact fibrous (i.e. stromal and epithelial) breast tissue, epithelial organoids isolated by collagenase digestion, cultured epithelial organoids, and cultured fibroblasts from reduction mammoplasty specimens.

We have collected snap-frozen human breast samples from nulliparous or parous patients who had either undergone reduction mammoplasty or had an excisional biopsy for a lesion that was ultimately determined to be benign (and not associated with elevated breast cancer risk). Tissue was taken from regions determined to be normal, as assessed by a breast pathologist.

Next, we isolated RNA from these tissues, and identified samples with intact RNA (Figure 1). All of these samples yielded RNA of sufficient quality for Affymetrix analysis, and were used to determine the global gene expression profiles of parous and nulliparous mammary glands in Task 6.

Efforts to procure additional specimens and harvest quality, intact RNA from these samples are on-going. These continuing efforts will provide us with adequate numbers of samples for identifying genes that correlate with reproductive history via

Affymetrix gene expression analysis (Tasks 6 and 7).

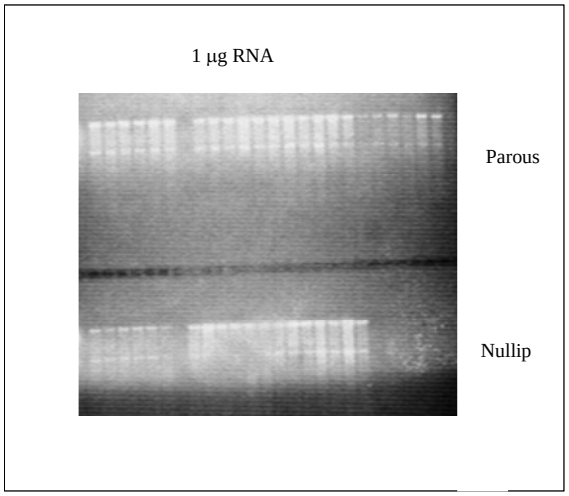

Figure 1. Ethidium bromide-stained gel of representative RNA samples from nulliparous and parous normal breast tissue samples illustrating that RNA is intact.

Task 6: Months 3-52: Determine global gene expression profiles for human mammary gland samples using oligonucleotide microarrays.

Per the SOW, work on this aim has been initiated and progress has been made. Biotinylated cRNA has been prepared from a subset of the RNA samples isolated in Task 5 and proof-of-principle experiments have been performed to demonstrate that these samples can be run on Affymetrix microarrays and meet established quality control standards.

Tissue samples with sufficient RNA yields and quality were labeled according to manufacturer's protocol for hybridization to Affymetrix U133A GeneChips. Following labeling and hybridization to microarrays, 72 samples (22 nulliparous, 50 parous) passed QC inspection and were appropriate for analysis.

We are continuing this task by isolating RNA from additional human specimens (Task 5), and upon obtaining quality RNA, hybridizing these samples to U133A GeneChips. These continuing efforts will provide us with adequate numbers of samples for identifying genes that correlate with reproductive history via Affymetrix gene expression analysis (Task 7).

Task 7: Months 12-60: Identify genes whose expression in the mammary gland in women reflects aspects of reproductive history that impact on breast cancer susceptibility.

Per the SOW, work on this task has continued in the previous study period. To date, the relatively small number of arrays that have been run, and the large number of reproductive variables that need to be analyzed, has precluded the identification of any genes. These will presumably emerge as these studies proceed over the next three study periods. Despite this, our preliminary results are summarized below.

As a preliminary approach, we explored the use of principal component analysis (PCA) to provide an initial overview of these samples. PCA uses the most variant genes

in a dataset (~6700 for this dataset), and projects data within a virtual three dimensional space based on gene expression. The first two components typically reflect the most robust differences in gene expression among samples. Breast samples for nulliparous (green) and parous (pink) microarrays did not appear to be distinguishable on the basis of the first two components by PCA (Fig. 2). This finding suggests that reproductive history does not explain the most predominant inter-patient differences in gene expression. Incidentally, in analogous studies using rodent samples, parity-induced gene changes typically predominant the first two components of a PCA, rendering nulliparous and parous samples into unique gene expression space.

We are currently attempting to identify those genes that contribute to these principal components. As we obtain additional human specimens, prepare RNA, and perform Affymetrix gene expression analysis, our ability to identify genes whose expression correlates with reproductive status may improve. In addition, we are planning to employ other analytical methods to identify these genes, such as expression deconvolution, that allows us to correct for differences in tissue compartments among samples.

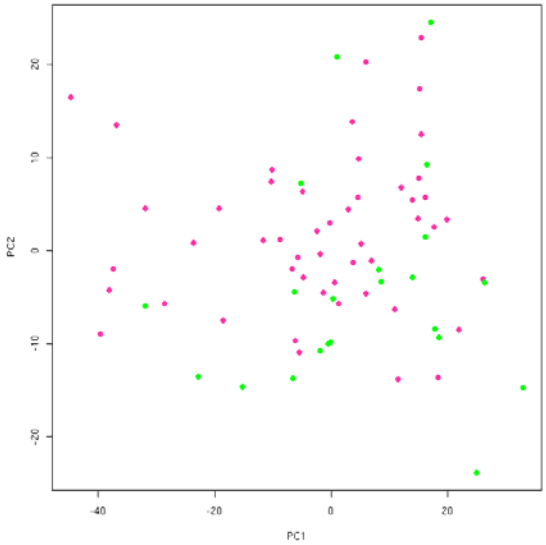

Figure 2: Principal Component Analysis based on the expression of ~6700 variant probe sets demonstrates that nulliparous (green) and parous (pink) samples do not separate by the first 2 components, suggesting that reproductive history is not the largest discriminator for this data set.

Task 8: Months 1-36: Determine the effect of short-term, low-dose estradiol and progesterone treatment on MNU-induced mammary tumor susceptibility.

This task has been completed on schedule. To determine whether lower doses of estradiol and progesterone confer protection against MNU-induced tumorigenesis, rats were treated with MNU followed by various doses of estradiol or estradiol plus progesterone. As expected, treatment of rats with 35mg estradiol plus 35mg progesterone for 3 weeks led to reduced MNU-induced mammary tumor susceptibility; this dose has previously been shown to confer protection against tumorigenesis (Figure 3). Reducing the dose of estradiol to 500ug (Figure 3) or 250ug (Figure 4) for 3 weeks also conferred protection, either alone or in conjunction with 35mg progesterone. To determine whether shorter hormone treatment time can also reduce tumor susceptibility, rats were treated

with MNU followed by 500ug estradiol for just 1 week. This treatment also conferred protection against mammary tumors (Figure 3). Thus these results indicate that short-term, low-dose estradiol leads to a reduction in susceptibility to MNU-induced mammary tumors.

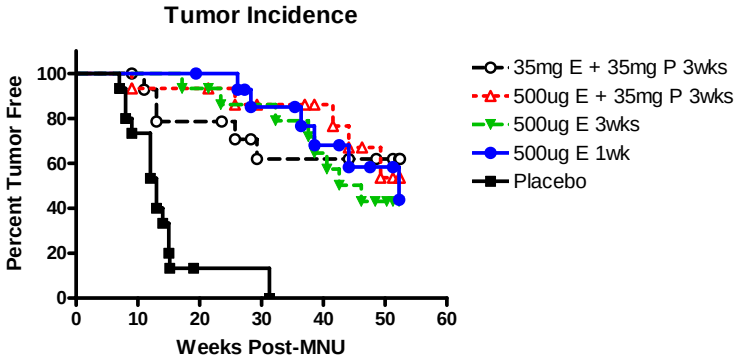

	500ug E + 35mg P 3wks	500ug E 3wks	500ug E 1wk	Placebo
35mg E + 35mg P 3wks	0.7962	0.7200	0.9254	0.0002
500ug E + 35mg P 3wks		0.4108	0.7963	<0.0001
500ug E 3wks			0.5345	<0.0001
500ug E 1wk				<0.0001

Figure 3. Short-term and low-dose (500ug) estradiol treatment confers protection against MNU-induced mammary tumorigenesis.

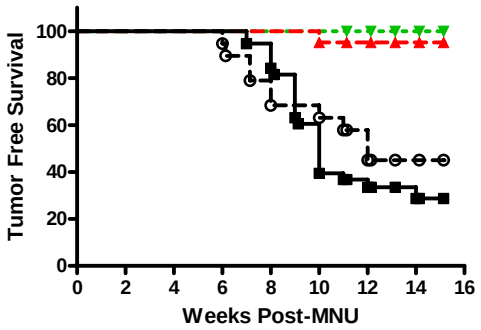

P-values

	E+P	P	AMV
E	.3545	.0003	<.0001
E+P		.0007	<.0001
P			.4123

Figure 4. Low-dose (250ug) estradiol treatment confers protection against MNU-induced mammary tumorigenesis.

Task 9: Months 12-60: Determine the effect of hormone treatment on MNU-induced mammary epithelial proliferation.

This task has been temporarily delayed to allow for progress toward and completion of other tasks, including tasks 8 and 10. Work on this task will continue during the next study period, consistent with the SOW.

Task 10: Months 12-60: Determine whether p53 loss abrogates pregnancy-induced protection against carcinogen-induced mammary tumorigenesis.

This task has been initiated and is proceeding according to the SOW. In order to address this aim, we first needed to demonstrate that the hormone-induced protection against tumors that has been observed in rats is also operative in mice. This is because mice, but not rats, offer the opportunity to use genetic knockouts, which is the preferred approach for addressing the involvement of p53 in pregnancy-induced protection.

To determine whether mice also exhibit hormone-induced protection, we first treated mice with estradiol plus progesterone (E+P) for 21 days beginning at 4 weeks of age, followed by weekly DMBA administration from 8 to 14 weeks to induce tumorigenesis. We tested 2 strains—BALBc/J mice, which have been shown by the Medina lab to be afforded protection by hormone treatment, and FVB mice, which is the strain used for many knockout studies in many laboratories, including our own. E+P treatment did not delay mammary tumorigenesis in either strain, and actually accelerated tumorigenesis in FVB mice (Figure 5).

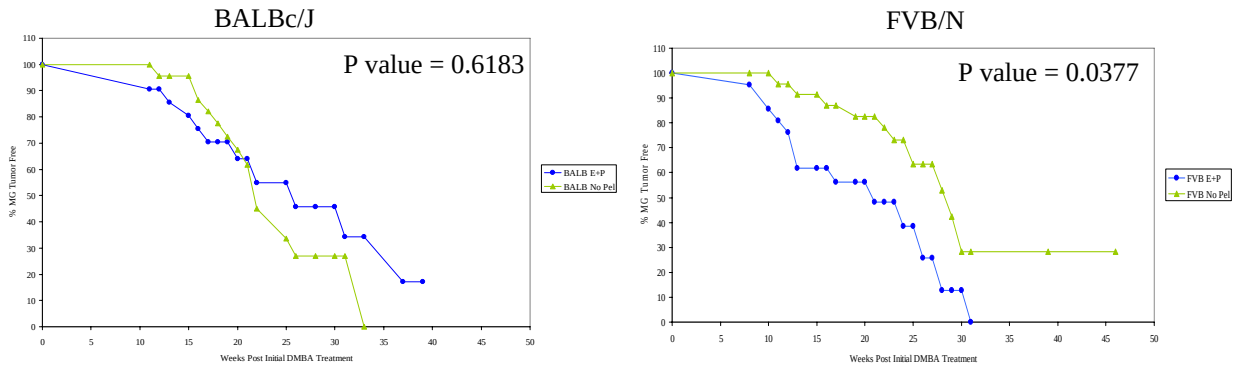

Figure 5. E+P treatment does not delay DMBA-induced mammary tumorigenesis in either BALBc/J or FVB/N mice.

This result was unanticipated, given that the Medina lab had previously demonstrated that E+P treatment confers protection in BALBc mice. We considered the possibility that the substrain of BALBc mice we used may have differed from the substrain they used, given that they have maintained their BALBc colony for many years. To address this point, we obtained BALBc mice from the Medina lab and repeated the experiment. We found that, similar to our previous results, E+P treatment had no effect on DMBA-induced mammary tumorigenesis (Figure 6).

Finally, we tested whether E+P treatment can delay tumorigenesis initiated by expression of the Neu oncogene under the control of the MMTV promoter, as has been demonstrated by another laboratory. We treated MMTV-Neu mice with E+P for 21 days starting at 7 weeks of age and monitored tumor formation. Again, we found that hormone treatment had no effect on mammary tumorigenesis driven by the Neu oncogene (Figure 7).

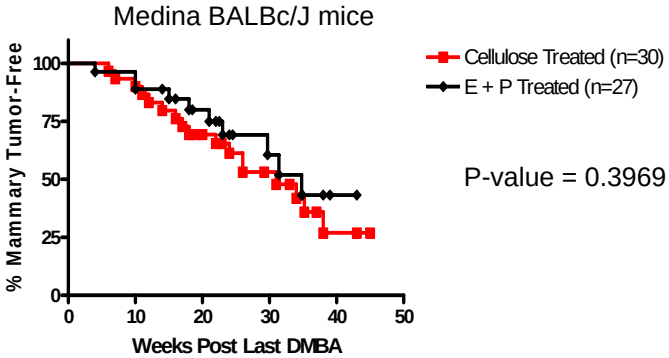

Figure 6. E+P treatment does not delay DMBA-induced mammary tumorigenesis in the Medina substrain of BALBc/J mice.

To date all of our efforts to demonstrate parity- or hormone-induced protection against mammary tumorigenesis in mice have been unsuccessful. Given that this initial step is necessary for completing this task, we are continuing our efforts to identify an experimental paradigm in which protection can be observed in mice. Going forward, we plan to try different hormone dosing schedules, and feeding mice a diet with low phytoestrogens. These efforts will commence in the upcoming year.

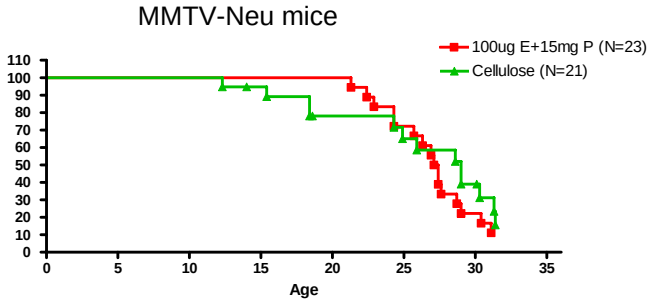

Figure 7. E+P treatment does not delay MMTV-Neu-induced mammary tumorigenesis.

Project 3

This project aims to recruit subjects being treated with a variety of hormonal regimens to have pre- and/or post-treatment breast biopsies. The treatment with the hormonal agents may or may not be a study procedure. A number of hormonal, genetic and cellular analyses will be carried out on the biopsy specimens obtained before and/or after the treatment regimen.

Task 1. Months 1-48: Develop appropriate protocols and treatment regimens.

To date we have developed five protocols directly related to this statement of work. The first two protocols are part of the approved statement of work and are described under Tasks 2a and 2b below. The three additional protocols are as follows:

The third protocol (first additional protocol) that has been developed involves obtaining breast biopsies from post-menopausal women who are receiving menopausal hormone therapy that contains micronized progesterone or placebo. This protocol has been approved by the USC IRB and recruitment has begun using non-DOD funds. We proceeded in this manner due to the extreme time delays that occur when submitting to the DOD IRB and the need to revise the SOW. We have enrolled 22 women into the study and plan to enroll an additional 18 women. We are in the process of preparing the DOD IRB submission and revised SOW to complete the analytic work for this protocol. We will evaluate the effect of these progestin doses on genetic and cellular characteristics of the breast tissue.

The fourth protocol that is in development involves obtaining breast biopsies from women donating eggs for *in vitro* fertilization. After follicle stimulation, these women achieve very high levels of estrogen at the time of egg donation and therefore we will be able to study the effects of pregnancy level estrogen in the absence of high progesterone levels. We plan to enroll 10 women in this protocol. It is currently under review by the USC IRB.

The fifth protocol which is directly related to this Innovator Award, but not funded through it, is our USC IRB-approved protocol which involves collecting breast tissue from women who have just had an induced abortion. This 'pregnant' breast tissue serves as an excellent comparator for the breast tissue that is been collected as part of Projects 3 and 4 (see below) or will be collected as part of the three protocols described above. In addition we have re-biopsied these women within one year of their original biopsy. We are in the process of preparing the DOD IRB submission and revised SOW to complete the analytic work for this protocol.

Task 2a. Recruit 10 women receiving high dose progestin (Megace) for the treatment of endometrial hyperplasia (as standard of care). For this research protocol, the subjects will receive a breast biopsy before Megace treatment, and after three months of Megace treatment.

We have developed this protocol which involves obtaining pre- and and post-treatment biopsies for women receiving high dose progestin for the treatment of endometrial hyperplasia. This protocol has been approved by both the USC and the DOD IRBs. The goal of the study is to recruit 10 women receiving high dose progestin (Megace) for the treatment of endometrial hyperplasia (as standard of care). We have consented five subjects for this protocol, three of whom have completed. We have recruitment procedures in place and expect to complete enrollment in the next nine months. For this research protocol, the subjects receive a breast biopsy before Megace treatment, and after three months of Megace treatment. We will evaluate the effect of this progestin on genetic and cellular characteristics of the breast tissue.

Task 2b. Recruit 40 women seeking oral contraceptives to be randomized to a low-dose progestin content oral contraceptive or a standard progestin content oral contraceptive and to have a breast biopsy after three months of oral contraceptive use

We have developed this protocol which involves obtaining breast biopsies from women randomized to two different progestin doses, but the same estrogen dose, of oral contraceptives. This protocol has been approved by the USC and DOD IRBs. The goal of this study is to recruit 40 women seeking oral contraceptives to be randomized to a low-dose progestin content oral contraceptive or a standard progestin content oral contraceptive and to have a breast biopsy after three month of oral contraceptive use. Enrollment of the

40 women in this protocol is complete and 24 women have completed the study. We will evaluate the effect of these progestin doses on genetic and cellular characteristics of the breast tissue.

As we continue to review the new literature and the results we generate we will develop additional protocols to further our understanding of how pregnancy provides long-term protection against breast cancer.

Task 3. Months 30-58: Assay tissue samples for hormonal, gene expression, and cellular markers to determine pre- and/or post-treatment tissue characteristics.

We are currently looking at MIB-1, ER, PR-A and PR-B in the samples collected through task 2b. We are currently processing all of the tissue collected through these protocols using laser capture microdissection to obtain clean cell populations. New improvements in technology have substantially reduced the amount of material needed for gene expression studies.

Task 4. Months 30-58: Assay blood samples for hormone levels.

We have provided the blood samples to the lab and this work is in process.

Task 5. Months 30-60: Conduct data analysis to compare pre- and/or post-treatment tissue characteristics, to compare these changes to the differences noted between nulliparous and parous women, and to prepare manuscripts as appropriate.

We will not begin this work for task 2a until we have enrolled the remaining subjects. We are currently awaiting results from the laboratory to begin analysis for task 2b with regard to cellular markers. We expect to have gene expression data in the next six to nine months and will begin that analysis.

We have completed one manuscript (attached) which compares cellular markers in the 'pregnant' breast tissue (fifth protocol described above) and the samples collected as part of Project 4 (see below). We observed profound differences in the pregnant breast tissue compared to non-pregnant breast tissue. PR-A expression was markedly reduced in the pregnant tissue and it appears that this decrease may endure for a few years after pregnancy. It is possible that short term changes in PR-A expression may be a marker of the effect of pregnancy on the breast. This could be used to monitor the effect of chemoprevention regimens aimed at mimicking the effect of pregnancy on the breast. This manuscript has been accepted by Breast Cancer Research and Treatment pending addressing reviewer comments.

Project 4

This project calls for the recruitment of 150 elective reduction mammoplasty patients. We will collect breast tissue from these women and conduct the same types of hormonal, genetic, and cellular analyses as will be done in Project 3. In addition, cellular analyses on 100 tissue slides from previous reduction mammoplasties will be conducted. In addition, cellular analyses will be conducted on 100 autopsy breast tissue samples. We are studying these three sources of breast tissue in parallel and thus describe our results to date together for these three tasks:

Task 1. Months 1-36: Recruit 150 women undergoing elective reduction mammoplasty to the protocol.

We have not been able to recruit any patients to this protocol in the past 12 months. This is because the number of patients being seen by our plastic surgeons for this procedure has decreased drastically. In order to address this issue we have written three new protocols designed to obtain normal breast tissue. We are revising the SOW accordingly. With these three new protocols we are planning to be on target to meet this goal.

The new protocols we have written include tissue collection from women undergoing a mastopexy procedure or a breast augmentation, and healthy volunteers. The mastopexy and breast augmentation protocols have been approved by the USC IRB and are ready to submit to the DOD IRB pending revision of the SOW. The healthy volunteer protocol has been approved by the USC IRB with contingencies which have already been addressed. This healthy volunteer protocol is similar to one that has been used by advocacy groups in Indiana to recruit hundreds of women for breast biopsies.

Task 1a. Months 1-36: Identify and conduct cellular assays on 100 tissue samples from previous reduction mammoplasties.

We are currently continuing to enroll women who previously had a reduction mammoplasty (Task 1a). We have identified 100 tissue samples and have detailed questionnaire data on 57 of the cases. We are reviewing the medical records of 43 additional women and anticipate being able to complete the cellular assays on these tissue within the next 12 months and thus this task will take until month 48 to complete enrollment.

Task 1b. Months 23-48: Identify and conduct cellular assays on 100 autopsy breast tissue samples.

We have obtained the 100 tissue samples and have found that the age of these samples affects the results of some of our cellular assays, in particular immunohistochemistry is not satisfactory. These samples are, however, adequate to better understand mammographic density. One of the secondary aims of this award is to better understand mammographic density as it is the strongest breast cancer risk factor.

These samples are those collected by Dr. Sue Bartow while working at the Office of the New Mexico Medical Investigator between December 1978 and December 1983. She collected randomly selected breast tissue from autopsied women (Bartow *et al*. 1997; Hart *et al.* 1989). Samples of this tissue from women without breast cancer was used by Dr. Norman Boyd and colleagues to measure constituents of the tissue (Li *et al.* 2005). Specifically from tissue slices which had been X-rayed (Faxitron) by Dr. Bartow and the Faxitron density measured (Faxitron percent density; Faxitron %), Dr. Boyd and colleagues obtained slides and measured the areas of the slide occupied by tissue (total area, TA), by collagen (collagen area, CA) and by epithelial nuclear material (epithelial nuclear area, ENA). From these measurements they calculated collagen percent (CP = 100 × CA/TA; Collagen %) and epithelial nuclear area percent (ENP = 100 × ENA/TA; Epithelial Nuclear Area %) and showed that Collagen % was highly correlated with Faxitron %. Dr. Boyd and colleagues kindly provided this data to us to allow us to investigate more fully the relationship between Collagen % and Epithelial Nuclear Area % and how they relate to other personal data that Dr. Bartow had been able collected on the women in the study. Fig. 1 shows the very close relationship between Collagen % and Faxitron %. Mammographic (Faxitron) densities essentially represent the collagen content of the breast.

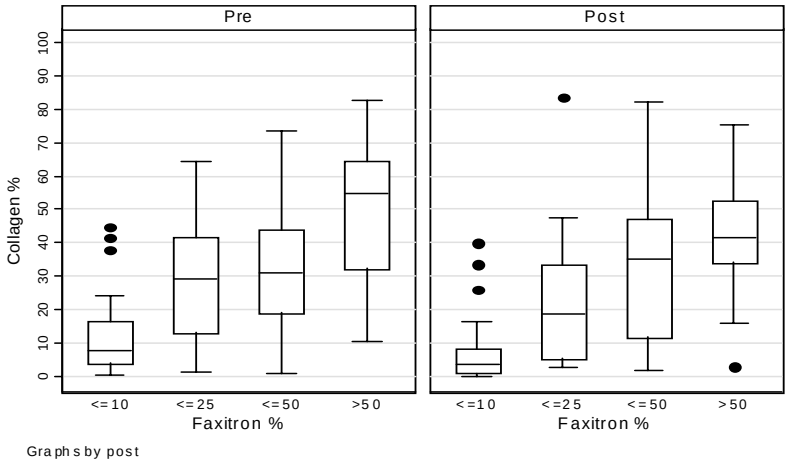

Figure 1. Relation of Collagen % to Faxitron % in premenopausal (Pre) and postmenopausal (Post) women.

We previously showed (Hawes *et al.* 2006) as part of this grant that a very high proportion of breast epithelial tissue is contained within dense collagen areas. Fig. 2 shows the correlation of Epithelial Nuclear Area % and Collagen %, confirming the relationship we found previously (Hawes *et al.* 2006). The relationship is clearly different in premenopausal compared to postmenopausal women. There is much less Epithelial Nuclear Area % per Collagen % in postmenopausal women than in premenopausal women. Within each menopausal category, there is a linear relationship through the origin (*i.e.* a proportional relationship) between Epithelial Nuclear Area % and Collagen %. The proportional (percentage) relationship can be written

$$PENC = 100 \times ENP/CP$$

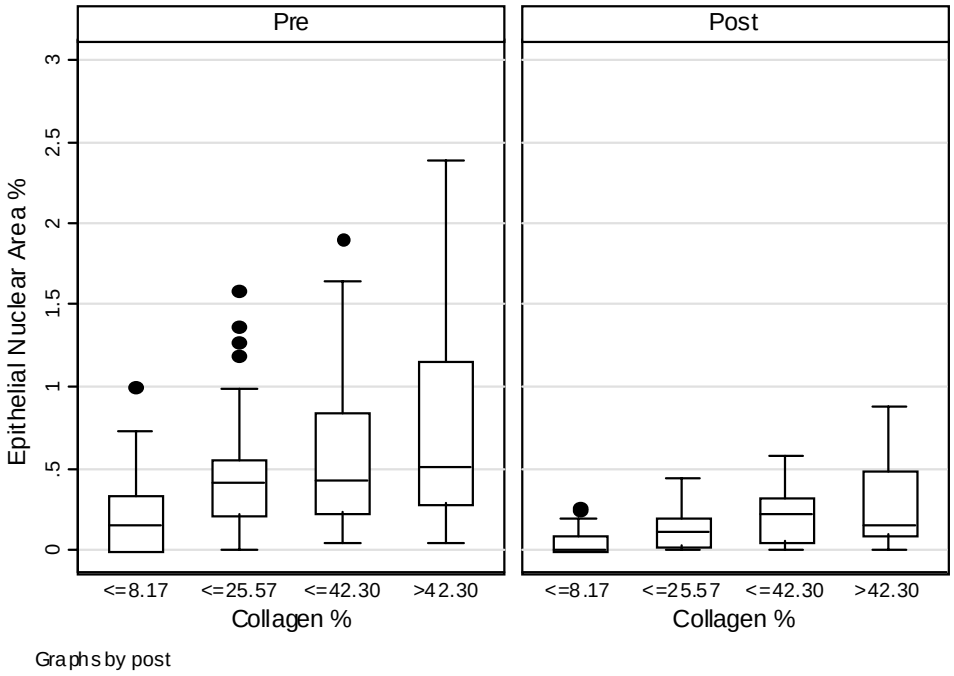

Figure 2. Relation of Epithelial Nuclear Area % to Collagen % in premenopausal (Pre) and postmenopausal (Post) women.

The strongest 'environmental' factor influencing mammographic densities is parity. Mammographic densities are steadily reduced with each birth, as is long-term breast cancer risk. An important question to ask is whether the concentration of epithelium in collagen (*i.e.*, PENC) is affected by births. If the amount of breast epithelium is not affected by parity then PENC will increase with births due to the decrease in collagen (mammographic density) with births. Initial analysis suggests that as densities (collagen) decrease, epithelium decreases but to a smaller extent. This provides a fundamental insight into the mechanism of the protective effect of births against breast cancer, namely, births may decrease the tissue (epithelium) at risk. Detailed analysis is ongoing and a manuscript describing these findings will shortly be prepared for submission for publication.

Task 2. Months 5-48: Assay tissue samples for hormonal and cellular markers to determine dense and non-dense tissue characteristics, and their association with glandular tissue proliferation.

We have assayed the tissue for a series of hormonal and cellular markers. To date, we have characterized ER expression, PR-A expression, PR-B expression, as well as quantified cell proliferation in the samples collected as part of Tasks 1 and 1a. A manuscript of these results has been accepted by Breast Cancer Research and Treatment (attached) pending response to the reviewer comments.

Task 3. Months 5-48: Assay blood samples for hormone levels.

We have provided the samples to the lab for hormone analysis.

Task 4. Months 37-48: Conduct gene expression arrays on the dense and non-dense tissue samples to determine if the expression profiles differ.

We are currently completing laser capture microdissection to obtain clean cell populations of epithelial cells and stroma (dense tissue). We expect to complete this task on target.

Task 5. Months 13-60: Conduct data analysis to compare dense and non-dense tissue characteristics and prepare manuscripts as appropriate.

We are continuing to analyze the data we have collected and have had one manuscript accepted pending revisions by Breast Cancer Research and Treatment (attached) and we are currently writing the manuscript of the data described above in task 1b.

KEY RESEARCH ACCOMPLISHMENTS:

- Treatment of rats with hormonal chemoprevention regimens and determination of effective regimens.
- Evaluation of rat mammary gland morphology.
- Identification of genes expressed in a parity-specific manner in multiple rat strains resulting in a key publication (Blakely *et al., Cancer Research,* 66:6421-6431, 2006; erratum in 67:844-846).
- Development and initiation of a protocol to allow us to evaluate the appropriateness of a progestin-based breast cancer chemopreventive approach.
- Development and initiation of a protocol to collect interview data, tissue specimens, and mammograms on women having elective reduction mammoplasties.
- Development of a protocol to allow us to evaluate breast cell proliferation in women receiving different progestin-dose oral contraceptives.
- Development of a protocol to allow us to evaluate breast cell proliferation in women receiving micronized progesterone versus placebo to determine the effect of exogenous progesterone on proliferation.
- Development of a protocol to allow us to evaluate the effects of high dose estrogen on breast tissue.
- Development of a protocol to allow us to collect breast tissue from women undergoing mastopexy procedures.
- Development of a protocol to allow us to collect breast tissue from women receiving a breast augmentation.
- Development of a protocol to allow us to collect breast tissue from healthy volunteers.
- Discovery that collagen is produced in both stromal and epithelial cells.
- Evaluation of tissue samples from reduction mammoplasties resulting in a seminal publication (Hawes *et al., Breast Cancer Research,* 8:R24-29, 2006).
- Contact and interview 22 additional previous reduction mammoplasty subjects to obtain demographic, reproductive, and hormone use data.
- Identify remaining 43 previous reduction mammoplasty subjects to obtain demographic, reproductive and hormone use data.
- Staining and evaluation of ER-A, PR-A, and PR-B expression and cell proliferation in previous reduction mammoplasty samples and prospective reduction mammoplasty samples.
- Discovery of a sustaining decrease in PR-A after pregnancy as a potential marker of the protective effect of pregnancy on breast cancer risk (Taylor *et al.*, in review).
- Development of methods for laser capture microscopy (LCM) to isolate relevant cell populations.
- Successful RNA extraction, quantitation and integrity evaluation from LCM sample followed by quantitative gene expression measurement of both high and low abundance markers.
- A further key accomplishment is the development of a network of collaborators at USC and across the United States to further the work being funded by this grant.
    - At USC we continue to have lively bi-monthly meetings of our working group of investigators with expertise in endocrinology, gynecology, breast

cancer pathology, oncology, radiology, epidemiology and molecular biology/embryology who meet at least twice a month to review progress of the various projects and specific related tasks and to discuss any data generated from the studies and any new questions that may arise from our studies or published literature.

- We continue to have fruitful collaborations with Dr. Sue Bartow for studies on breast specimens from autopsies performed in New Mexico. These are the same specimens utilized by Dr. Norman Boyd's group (Li *et al.*, *Cancer Epidemiol Biomarkers Prev*, 14:343-349, 2005) and we are collaborating with Dr. Boyd to analyze these data further.

- Demonstration that low-dose and short-term hormone treatment of rats reduces mammary tumor susceptibility.
- Extensive attempts to recapitulate hormone and parity-induced protection against mammary tumorigenesis in mice.

REPORTABLE OUTCOMES:

1. Blakely CM, Stoddard AJ, Belka GK, Dugan KD, Notarfrancesco KL, Moody SE, D'Cruz CM, and Chodosh LA. Hormone-induced protection against mammary tumorigenesis is conserved in multiple rat strains and identifies a core gene expression signature induced by pregnancy. *Cancer Research*, 66:6421-6431, 2006; erratum in 67:844-846.
2. Hawes D, Downey S, Pearce CL, Bartow S, Wan P, Pike MC, Wu AH. Dense breast stromal tissue shows greatly increased concentration of breast epithelium but no increase in its proliferative activity. *Breast Cancer Res*, 8:R24-29, 2006.
3. Taylor D, Pearce CL, Hovanessian-Larsen L, Downey S, Spicer DV, Bartow S, Ling C, Pike MC, Wu AH, Hawes D. Progesterone and estrogen receptors in pregnant and premenopausal non-pregnant normal human breast. Provisionally accepted by Breast Cancer Res Treat.

CONCLUSION:

Our finding that PR-A expression appears to be altered following pregnancy provides the first insight into a marker for mimicking the protective effect of a pregnancy on breast cancer risk. We are continuing to follow-up this work to determine if this change is induced in women who do not carry a pregnancy to term.

Our finding that breast epithelial tissue in women is overwhelmingly concentrated in mammographically dense areas of the breast (areas of high collagen concentration not seen in rodent breast) provides a deep insight into the reason for increased mammographic density being so closely associated with increased risk of breast cancer - women with increased mammographic density have more breast epithelium. The reason(s) for this relationship is at present unclear and is a focus of our current research. Breast densities are reduced in parous compared to nulliparous women, so that this endeavor ties in closely with our development of a chemoprevention regimen to mimic the protective effect of pregnancy. It may be that the genetic expression changes brought about by pregnancy (discussed above) are themselves responsible for the reduction in densities.

In addition, through our successful development of a laser capture microscopy protocol and new technology which reduces the amount and quality of RNA needed for these studies will enable us to conduct large scale gene expression studies on the relevant breast cell populations over the next year and we hope it will provide further insight into the characteristics of the parous breast which ultimately provides protection against breast cancer.

REFERENCES:

1. Bartow SA, Mettler FA, Black WC. Correlations between radiographic patterns and morphology of the female breast. *Rad Patterns Morph*, 13:263-275, 1997.
2. Blakely CM, Stoddard AJ, Belka GK, Dugan KD, Notarfrancesco KL, Moody SE, D'Cruz CM, and Chodosh LA. Hormone-induced protection against mammary tumorigenesis is conserved in multiple rat strains and identifies a core gene expression signature induced by pregnancy. *Cancer Research*, 66:6421-6431, 2006; erratum in 67:844-846.
3. Hart BL, Steinbock RT, Mettler FA Jr, Pathak DR, Bartow SA. Age and race related changes in mammographic parenchymal patterns. *Cancer*, 63:2537-2539, 1989.
4. Hawes D, Downey S, Pearce CL, Bartow S, Wan P, Pike MC, Wu AH. Dense breast stromal tissue shows greatly increased concentration of breast epithelium but no increase in its proliferative activity. *Breast Cancer Res*, 8:R24-29, 2006.
5. Li T, Sun L, Miller N, Nicklee T,Woo J,Hulse-Smith L,Tsao MS,Khokha R, Martin L, Boyd N. *Cancer Epidemiol Biomarkers Prev,* 14:343-349, 2005.

APPENDICES:

1. List of personnel
2. Blakely CM, Stoddard AJ, Belka GK, Dugan KD, Notarfrancesco KL, Moody SE, D'Cruz CM, and Chodosh LA. Hormone-induced protection against mammary tumorigenesis is conserved in multiple rat strains and identifies a core gene expression signature induced by pregnancy. *Cancer Research*, 66:6421-6431, 2006; erratum in 67:844-846.
3. Hawes D, Downey S, Pearce CL, Bartow S, Wan P, Pike MC, Wu AH. Dense breast stromal tissue shows greatly increased concentration of breast epithelium but no increase in its proliferative activity. *Breast Cancer Res*, 8:R24-29, 2006.
4. Taylor D, Pearce CL, Hovanessian-Larsen L, Downey S, Spicer DV, Bartow S, Ling C, Pike MC, Wu AH, Hawes D. Progesterone and estrogen receptors in pregnant and premenopausal non-pregnant normal human breast. Provisionally accepted by Breast Cancer Res Treat.

Personnel List 2007-2008

University of Southern California – Projects 3 & 4

Malcolm C. Pike
Anna H. Wu
C. Leigh Pearce
Debra Hawes
Michael F. Press
Sue Ellen Martin
Frank Stanczyk
Jonathan Buckley
Lilly Chang
Alex Trana
Angela Umali
Peggy Wan
Lillian Young
Serina Ovalle
Yongtian Li
Randall Widelitz

University of Pennsylvania – Projects 1 & 2

Lewis H. Chodosh
Chien-Chung Chen
Celina D'Cruz
Congzhou Liu
Patrick Taulman
Jinling Wu
Dhruv Pant
Adanma Ezidinma

Hormone-Induced Protection against Mammary Tumorigenesis Is Conserved in Multiple Rat Strains and Identifies a Core Gene Expression Signature Induced by Pregnancy

Collin M. Blakely, Alexander J. Stoddard, George K. Belka, Katherine D. Dugan, Kathleen L. Notarfrancesco, Susan E. Moody, Celina M. D'Cruz, and Lewis A. Chodosh

Departments of Cancer Biology, Cell and Developmental Biology, and Medicine, and The Abramson Family Cancer Research Institute, University of Pennsylvania School of Medicine, Philadelphia, Pennsylvania

Abstract

Women who have their first child early in life have a substantially lower lifetime risk of breast cancer. The mechanism for this is unknown. Similar to humans, rats exhibit parity-induced protection against mammary tumorigenesis. To explore the basis for this phenomenon, we identified persistent pregnancy-induced changes in mammary gene expression that are tightly associated with protection against tumorigenesis in multiple inbred rat strains. Four inbred rat strains that exhibit marked differences in their intrinsic susceptibilities to carcinogen-induced mammary tumorigenesis were each shown to display significant protection against methylnitrosourea-induced mammary tumorigenesis following treatment with pregnancy levels of estradiol and progesterone. Microarray expression profiling of parous and nulliparous mammary tissue from these four strains yielded a common 70-gene signature. Examination of the genes constituting this signature implicated alterations in transforming growth factor-β signaling, the extracellular matrix, amphiregulin expression, and the growth hormone/insulin-like growth factor I axis in pregnancy-induced alterations in breast cancer risk. Notably, related molecular changes have been associated with decreased mammographic density, which itself is strongly associated with decreased breast cancer risk. Our findings show that hormone-induced protection against mammary tumorigenesis is widely conserved among divergent rat strains and define a gene expression signature that is tightly correlated with reduced mammary tumor susceptibility as a consequence of a normal developmental event. Given the conservation of this signature, these pathways may contribute to pregnancy-induced protection against breast cancer. (Cancer Res 2006; 66(12): 6421-31)

Introduction

Epidemiologic studies clearly show that a woman's risk of developing breast cancer is influenced by reproductive endocrine events (1). For example, early age at first full-term pregnancy, as well as increasing parity and duration of lactation, have each been shown to reduce breast cancer risk (2, 3). In particular, women who have their first child before the age of 20 have up to a 50% reduction in lifetime breast cancer risk compared with their nulliparous counterparts (2). Notably, the protective effects of an early full-term pregnancy have been observed in multiple ethnic groups and geographic locations, suggesting that parity-induced protection results from intrinsic biological changes in the breast rather than specific socioeconomic or environmental factors. At present, however, the biological mechanisms underlying this phenomenon are unknown.

Several models to explain the protective effects of parity have been proposed. For instance, parity has been hypothesized to induce the terminal differentiation of a subpopulation of mammary epithelial cells, thereby decreasing their susceptibility to oncogenesis (4). Related to this, parity has been suggested to induce changes in cell fate within the mammary gland, resulting in a population of mammary epithelial cells that are more resistant to oncogenic stimuli by virtue of decreased local growth factor expression and/or increased transforming growth factor (Tgf)-β3 and p53 activity (5, 6). Others have suggested that the process of involution that follows pregnancy and lactation acts to eliminate premalignant cells or cells that are particularly susceptible to oncogenic transformation (5). Conversely, parity-induced decreases in breast cancer susceptibility could also be due to persistent changes in circulating hormones or growth factors rather than local effects on the mammary gland (7). At present, however, only limited cellular or molecular evidence exists to support any of these models.

Similar to humans, both rats and mice exhibit parity-induced protection against mammary tumorigenesis. Administration of the chemical carcinogens, 7,12-dimethylbenzanthracene or methylnitrosourea, to nulliparous rats results in the development of hormone-dependent mammary adenocarcinomas that are histologically similar to human breast cancers (8). In outbred Sprague-Dawley, and inbred Lewis and Wistar-Furth rats, a full-term pregnancy either shortly before or after carcinogen exposure results in a high degree of protection against mammary carcinogenesis (7, 9, 10). Similarly, treatment of rats with pregnancy-related hormones, such as 17-β-estradiol (E) and progesterone (P), can mimic the protective effects of pregnancy in rat mammary carcinogenesis models (11, 12). This suggests that the mechanisms of parity-induced protection and estradiol and progesterone–induced protection may be similar. Using analogous approaches, Medina and colleagues have shown parity-induced as well as hormone-induced protection against 7,12-dimethylbenzanthracene–initiated carcinogenesis in mice (13, 14). As such, rodent models recapitulate the ability of reproductive endocrine events to modulate breast cancer risk as observed in humans. This, in turn, permits the mechanisms of parity-induced protection to be studied within defined genetic and reproductive contexts.

Requests for reprints: Lewis A. Chodosh, Department of Cancer Biology, University of Pennsylvania School of Medicine, 612 Biomedical Research Building II/III, 421 Curie Boulevard, Philadelphia, PA 19104-6160. Phone: 215-898-1321; Fax: 215-573-6725; E-mail: chodosh@mail.med.upenn.edu.

doi:10.1158/0008-5472.CAN-05-4235

Previously, analyses of gene expression changes that occur in rodent models in response to parity, or hormonal treatments that mimic parity, have been used to suggest potential cellular and molecular mechanisms for pregnancy-induced protection against breast cancer (6, 15). Rosen and colleagues used subtractive hybridization analysis to identify genes in the mammary glands of Wistar-Furth rats that were persistently up-regulated 4 weeks posttreatment with estradiol and progesterone (15). Estradiol and progesterone treatment was found to increase the mRNA expression of a wide range of genes, including those involved in differentiation, cell growth, and chromatin remodeling. Similarly, we used microarray expression profiling to assess global gene expression changes induced by parity in the mammary glands of FVB mice (6). This analysis revealed parity-induced increases in epithelial differentiation markers, *Tgfb3* and its downstream targets, and cellular markers reflecting the influx of macrophages and lymphocytes into the parous gland. We also found that parity resulted in persistent decreases in the expression of a number of growth factor–encoding genes, including amphiregulin (*Areg*) and insulin-like growth factor (*Igf-I*). Together, these studies provided initial insights into cellular and molecular mechanisms that could contribute to parity-induced protection.

Notably, early first full-term pregnancy in humans primarily decreases the incidence of estrogen receptor (ER)-positive breast cancers (16). Because rats are more similar to humans than are mice with respect to the incidence of ER-positive mammary tumors (17), in the present study we used microarray expression profiling to identify persistent gene expression changes in the mammary glands of this rodent species to explore potential mechanisms of parity-induced protection. To date, a comprehensive analysis of parity-induced up-regulated and down-regulated gene expression changes in the rat has not been performed.

A major challenge posed by global gene expression surveys is the large number of differentially expressed genes that are typically identified, only a few of which may contribute causally to the phenomenon under study. Consequently, we considered approaches to identifying parity-induced changes in the rat mammary gland that would permit the resulting list of expressed genes to be narrowed to those most robustly associated with parity-induced protection against mammary tumorigenesis. Given the marked genetic and biological heterogeneity between different inbred rat strains, we reasoned that identifying expression changes that are conserved across multiple strains exhibiting hormone-induced protection against mammary tumorigenesis would facilitate the identification of a core set of genes associated with parity-induced protection against breast cancer.

To achieve this goal, we focused on gene expression changes that are conserved among different strains of rats that exhibit hormone-induced protection against mammary tumorigenesis. We first identified four genetically distinct inbred rat strains that exhibit hormone-induced protection against methylnitrosourea-induced mammary tumorigenesis independent of their inherent susceptibility to this carcinogen. We then used oligonucleotide microarrays to identify a core 70-gene expression signature that closely reflects parity-induced changes in the mammary gland that were conserved among each of these strains. The results of this analysis extend prior observations with respect to parity-induced changes in the growth hormone/Igf-I axis, identify novel parity-induced changes associated with the extracellular matrix (ECM), and implicate a core set of pathways in pregnancy-induced protection against breast cancer.

Materials and Methods

Animals and tissues. Lewis, Wistar-Furth, Fischer 344, and Copenhagen rats (Harlan, Indianapolis, IN) were housed under 12-hour light/12-hour dark cycles with access to food and water ad libitum. Animal care was performed according to institutional guidelines. To generate parous (G1P1) rats, 9-week-old females were mated and allowed to lactate for 21 days after parturition. After 28 days of postlactational involution, rats were sacrificed by carbon dioxide asphyxiation and the abdominal mammary glands were harvested and snap-frozen following lymph node removal, or whole-mounted and fixed in 4% paraformaldehyde. Whole-mounted glands were stained with carmine alum as previously described (6). For histologic analysis of whole mammary glands and tumors, paraffin-embedded tissues were sectioned and stained with H&E or Mason's trichrome as previously described (6). Tissues were harvested from age-matched nulliparous (G0P0) animals in an identical manner.

Carcinogen and hormone treatments. Twenty-five to 30 nulliparous female Lewis, Fischer 344, Wistar-Furth, and Copenhagen rats were weighed and treated at 7 weeks of age with methylnitrosourea (Sigma-Aldrich, St. Louis, MO) at a dose of 50 mg/kg by a single i.p. injection. At 9 weeks of age, animals from each strain were assigned to one of two groups and treated with hormone pellets (Innovative Research, Sarasota, FL) by s.c. implantation. Group 1 received pellets containing 35 mg of 17-β-estradiol + 35 mg of progesterone, whereas group 2 received pellets containing placebo. Pellets were removed after 21 days of treatment. No signs of toxicity were observed. The development of mammary tumors was assessed by weekly palpation. Animals were sacrificed at a predetermined tumor burden, or at 60 weeks postmethylnitrosourea. At sacrifice, all mammary glands were assessed for tumors, which were fixed in 4% paraformaldehyde and embedded in paraffin. Tumor samples from each strain were confirmed as carcinomas by histologic evaluation. Statistical differences in tumor-free survival between experimental groups were determined by log rank tests and by the generation of hazard ratios (HR) based on the slope of the survival curves using GraphPad Prism 4.0 software.

Microarray analysis. RNA was isolated from snap-frozen abdominal mammary glands by the guanidine thiocyanate/cesium chloride method as previously described (6). Ten micrograms of total RNA from individual Wistar-Furth (six G0P0 and five G1P1), Fischer 344 (eight G0P0 and six G1P1), and Copenhagen (six G0P0 and five G1P1) rats was used to generate cDNA and biotinylated cRNA as previously described (6). For Lewis rats, three G0P0 and three G1P1 samples were analyzed, each of which was comprised of 10 μg of pooled RNA from three animals. To permit the identification of epithelial as well as stromal gene expression changes, intact mammary glands (with lymph nodes removed) were used. Samples were hybridized to high-density oligonucleotide microarrays (RGU34A) containing ~8,800 probe sets representing ~4,700 genes and expressed sequence tags. Affymetrix comparative algorithms (MAS 5.0) and Chipstat were used to identify genes that were differentially expressed between nulliparous and parous samples (18). Robust Multichip Average signal values were generated using Bioconductor (19).

Genes were selected for further analysis whose expression changed significantly by the above analysis in three out of four strains. Significance was assessed by randomly generating eight lists equal in size to the up-regulated and down-regulated lists for each strain from the population of nonredundant genes called present on the chip in at least one sample (2,428 genes). One million random draw trials were performed to calculate a nominal *P* value for combined list length and to estimate the false discovery rate (FDR) using the median list size occurring by chance.

Hierarchical clustering was done using R statistical software[1] and as described (20). Mouse genes were identified using the Homologene database (National Center for Biotechnology Information).

Quantitative real-time PCR. Five micrograms of DNase-treated RNA were used to generate cDNA by standard methods. *Csn2, Mmp12, Tgfb3,*

[1] http://www.R-project.org.

Igfbp5, Areg, Igf-I, Ghr, Serpinh1, and *Sparc* were selected for confirmation by quantitative real-time PCR (QRT-PCR) using TaqMan assays (Applied Biosystems, Foster City, CA). *B2m* was used as a control (21, 22). Reactions were performed in duplicate in 384-well microtiter plates in an ABI Prism Sequence Detection System according to standard methods (Applied Biosystems). One-tailed *t* tests were performed to determine statistical significance using Prism 4.0 software.

Results

Hormone-induced protection in inbred rat strains. To determine whether hormone-induced protection against mammary tumorigenesis is a feature unique to carcinogen-sensitive strains, we compared the extent of protection induced by hormones in four different rat strains: Lewis, Wistar-Furth, Fischer 344, and Copenhagen. Two of these strains (Lewis and Wistar-Furth) have been reported to exhibit hormone-induced protection (9, 12). However, it has not been determined whether carcinogen-resistant strains of rats, such as Copenhagen (23), also exhibit protection. Female rats from each strain were treated with a single dose of methylnitrosourea at 7 weeks of age, followed by s.c. implantation of either placebo or hormone pellets (35 mg of estradiol + 35 mg of progesterone) at 9 weeks of age. Among the placebo-treated groups, Lewis rats exhibited the highest susceptibility to methylnitrosourea-induced mammary tumorigenesis with 100% penetrance and a median tumor latency of 13 weeks (Fig. 1*A*). Fischer 344 and Wistar-Furth rats displayed intermediate carcinogen sensitivity with latencies of 24 and 36 weeks, respectively. In contrast, Copenhagen rats exhibited a high degree of resistance to methylnitrosourea-induced mammary tumorigenesis with only 5 of 12 animals developing mammary tumors, with an average latency of 51 weeks.

Surprisingly, despite the wide variance in carcinogen sensitivity of nulliparous rats from these four strains, estradiol and progesterone treatment induced a significant ($P < 0.05$) degree of protection against mammary tumorigenesis in each strain (Fig. 1*B*). For example, whereas Lewis and Copenhagen strains differed markedly in their sensitivity to methylnitrosourea, they exhibited strikingly similar degrees of hormone-induced protection with HRs of 0.19 [95% confidence interval (CI), 0.05-0.40] and 0.16 (95% CI, 0.02-0.63), respectively. The Wistar-Furth (HR, 0.31; 95% CI, 0.09-0.90) and Fischer 344 (HR, 0.38; 95% CI, 0.10-0.71) strains exhibited lesser, but significant degrees of protection. These experiments show that hormone treatments that mimic pregnancy confer protection against mammary tumorigenesis in each strain irrespective of the intrinsic carcinogen susceptibility of nulliparous animals from that strain.

Morphologic changes induced by parity in the rat mammary gland. Parity-induced changes in breast cancer susceptibility have been reported to be accompanied by persistent changes in the structure of the mammary gland in humans, as well as in rats and mice (4, 6). Consistent with this, carmine-stained whole-mount analysis of nulliparous and parous mammary glands from each of the four rat strains revealed that the architecture of the parous mammary epithelial tree was more complex than that of age-matched nulliparous animals, with a higher degree of ductal side-branching (Fig. 1*C*). These effects were observed in each of the four strains analyzed, suggesting that changes in the structural and cellular composition of the mammary gland may occur as a consequence of parity.

Microarray analysis of parity-induced changes in the rat mammary gland. The similar morphologic changes induced by parity suggested that the hormone-induced protection against mammary tumorigenesis that we observed in different rat strains might be accompanied by common molecular alterations. To identify these changes, we first performed oligonucleotide microarray expression profiling on pooled samples from nulliparous and parous Lewis rats. Genes whose expression changes were considered to be statistically significant using established algorithms, and whose expression changed by at least 1.2-fold as a result of parity, were selected for further analysis (18). This combined analytic approach has previously been shown to be capable of identifying differentially expressed genes with high sensitivity and specificity (18). Gene expression analysis performed in this manner identified 75 up-regulated and 148 down-regulated genes in parous compared with nulliparous mammary glands. Examination of this list of differentially expressed genes confirmed our previous findings in mice that parity results in the persistent up-regulation of *Tgfb3*, as well as differentiation and immune markers, as well as the persistent down-regulation of growth factor encoding genes, such as *Areg* and *Igf-I* (ref. 6; data not shown).

To narrow the list of candidate genes whose regulation might contribute to the protected state associated with parity, we attempted to identify parity-induced gene expression changes that were conserved across multiple rat strains. To this end, total RNA was isolated from the mammary glands of nulliparous and parous Wistar-Furth, Fischer 344, and Copenhagen rats, and analyzed on RGU34A arrays in a manner analogous to that employed for Lewis rats. This led to the identification of 68, 64, and 92 parity up-regulated genes and 132, 209, and 149 parity down-regulated genes in Wistar-Furth, Fischer 344, and Copenhagen rats, respectively.

Unsupervised hierarchical clustering performed using the expression profiles of 1,954 globally varying genes across the nulliparous and parous data sets representing the four rat strains revealed that samples clustered primarily based on strain without regard to parity status (Fig. 2*A*). This suggested that the principal source of global variation in gene expression across these data sets was due to genetic differences between strains rather than reproductive history. This observation suggested that determining which parity-induced gene expression changes were conserved among these highly divergent rat strains could represent a powerful approach to defining a parity-related gene expression signature correlated with hormone-induced protection against mammary tumorigenesis.

To identify parity-induced gene expression changes that were conserved across strains, we selected genes that exhibited $\geq$1.2-fold change in at least three of the four strains analyzed. This led to the identification of 24 up-regulated (Table 1) and 46 down-regulated genes (Table 2). Based on the number of parity-induced gene expression changes observed for each strain, an overlap of this size is highly unlikely by chance (up-regulated: $P < 1 \times 10^{-6}$, FDR < 1%; down-regulated: $P < 1 \times 10^{-6}$, FDR = 4%). As such, this approach led to the identification of 70 genes whose expression is persistently altered by parity across multiple strains of rats that exhibit hormone-induced protection against mammary tumorigenesis.

A gene expression signature distinguishes parous and nulliparous rats and mice. To confirm the validity of the 70-gene parity-related expression signature derived from the above studies, we performed oligonucleotide microarray analysis on samples from nulliparous and parous Lewis rats that were generated independently from those used to derive this signature. Hierarchical clustering analysis of these independent samples using the 70-gene signature revealed that the expression profiles of these genes were sufficient to accurately distinguish parous from nulliparous Lewis rat samples in a blinded manner (Fig. 2*B*).

To determine whether this parity-related signature could distinguish between nulliparous and parous mammary glands from multiple strains of rats, Lewis, Wistar-Furth, Fischer 344, and Copenhagen microarray data sets were clustered in an unsupervised manner based solely on the expression of the 70 genes comprising the parity signature (Fig. 2*C*). In each of the four rat strains examined, the 70-gene signature was sufficient to distinguish parous from nulliparous rats (Fig. 2*C*). Thus, this signature reflects parity-induced gene expression changes that are highly conserved among four genetically divergent rat strains.

Early full-term pregnancy has been reported to result in protection against mammary tumorigenesis in mice, as it does in humans and rats (13). Accordingly, we mapped the 70 genes

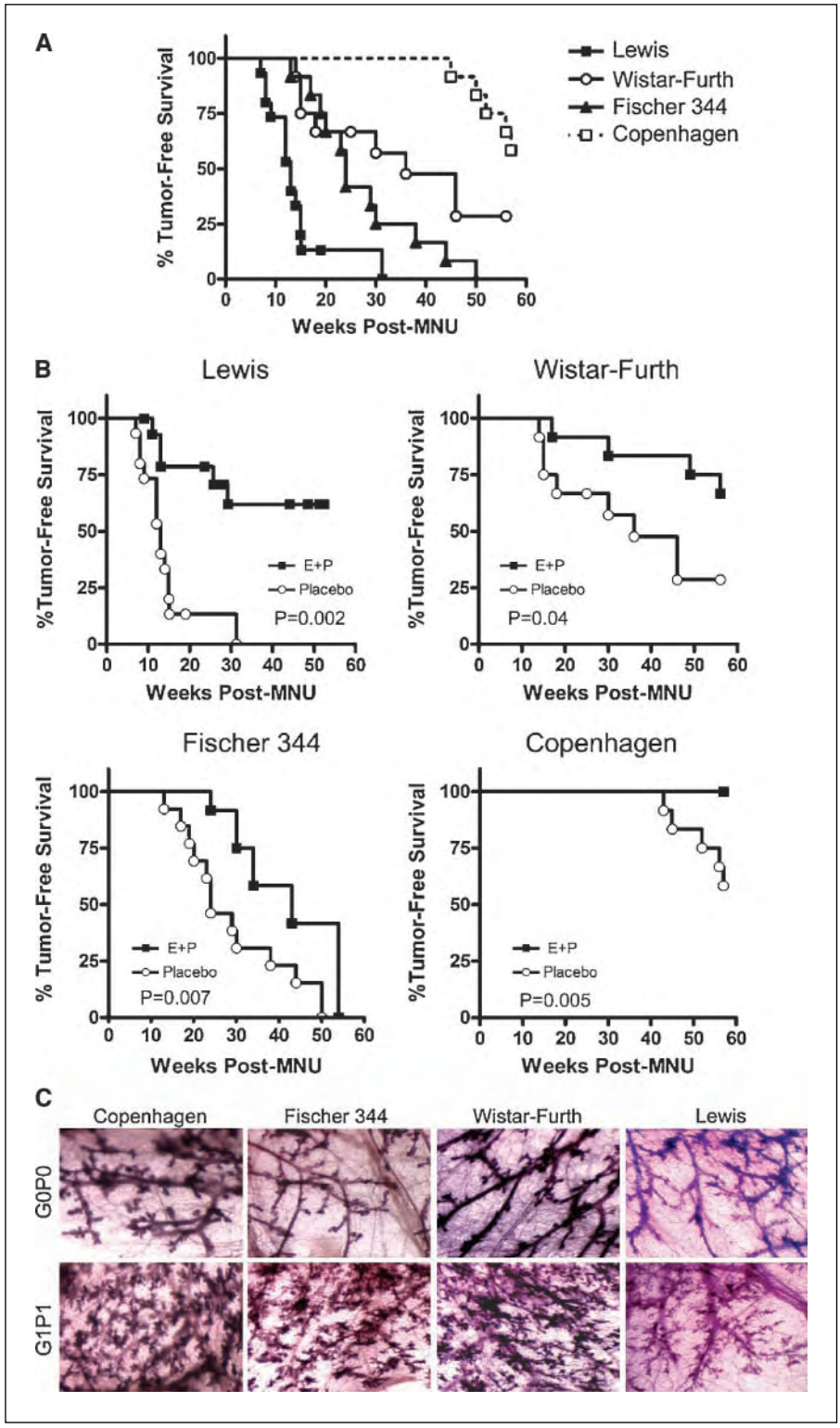

Figure 1. Hormone-induced protection against mammary tumorigenesis is conserved among multiple rat strains. *A,* Kaplan-Meier curves plotting the time to the formation of a first mammary tumor in placebo-treated groups for Lewis (n = 15), Wistar-Furth (n = 12), Fischer 344 (n = 13), and Copenhagen (n = 12) rats treated with methylnitrosourea (*MNU*) at 7 weeks of age. Significant differences in tumor incidence were identified between Lewis and Wistar-Furth (P = 0.0003), Lewis and Fischer 344 (P = 0.0005), Lewis and Copenhagen (P = 0.0001), Wistar-Furth and Copenhagen (P = 0.024), and Fischer 344 and Copenhagen (P = 0.0001) as determined by a log rank test. Wistar-Furth and Fischer 344 were not significantly different (P = 0.14). *B,* mammary tumor incidence for placebo and estradiol and progesterone–treated rats is plotted for each strain. Cohort sizes for estradiol and progesterone–treated animals were: Lewis (n = 16), Wistar-Furth (n = 12), Fischer 344 (n = 12), and Copenhagen (n = 12). Each strain exhibited significantly decreased tumor incidence in estradiol and progesterone–treated compared with placebo-treated cohorts. *C,* carmine-stained whole mounts of abdominal mammary glands from nulliparous (G0P0) and parous (G1P1) rats from each strain (original magnification, ×50). Samples are representative of three animals per group.

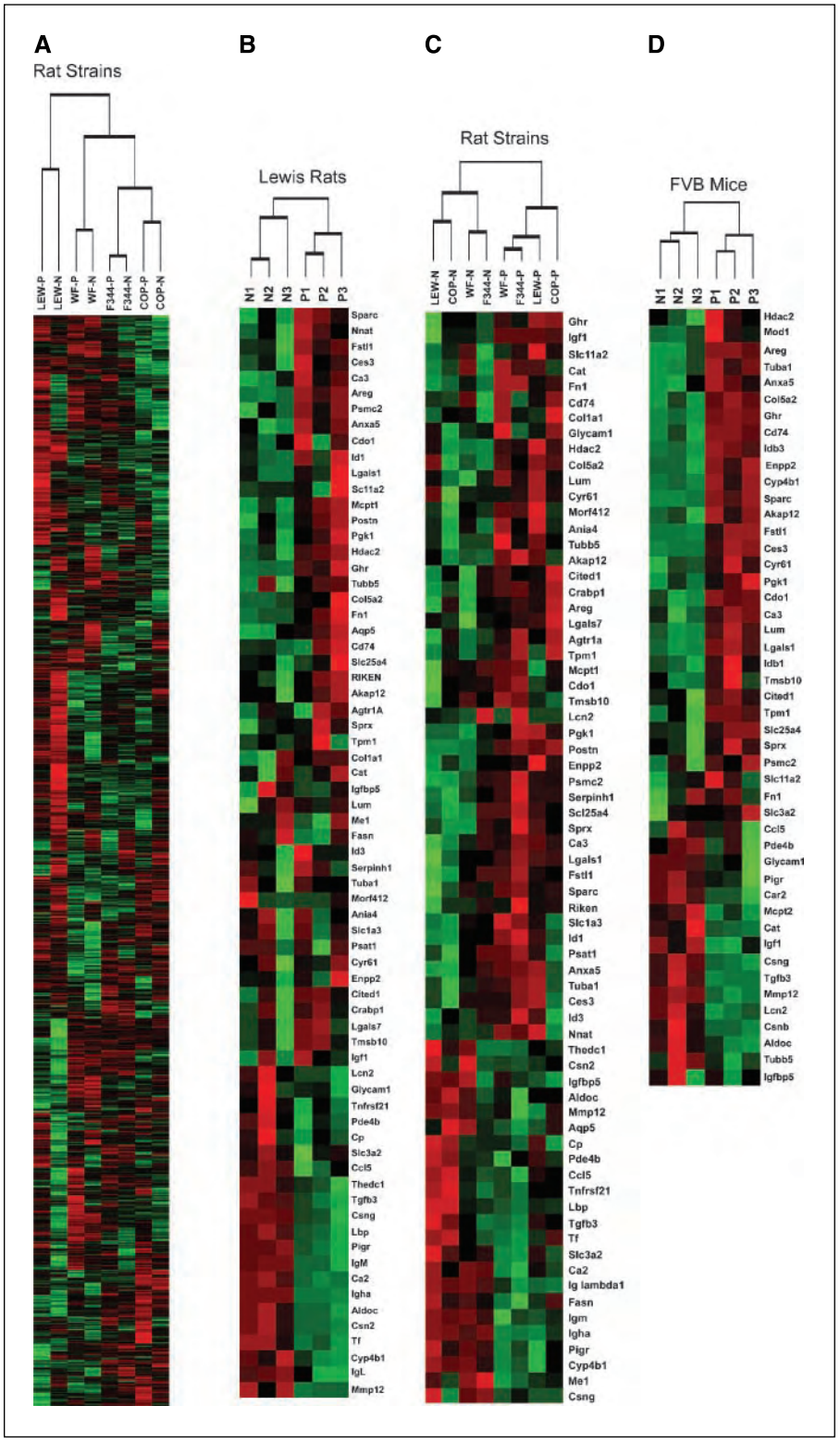

Figure 2. A parity-related gene expression signature distinguishes between nulliparous and parous rats and mice. Unsupervised hierarchical clustering analysis. Nulliparous (*N*), parous (*P*), Lewis (*LEW*), Fischer 344 (*F344*), Wistar-Furth (*WF*), and Copenhagen (*COP*). *A,* nulliparous and parous samples from each strain were clustered based on the median expression values of ~1,900 genes exhibiting global variation in gene expression across the data sets. *B,* six independent Lewis samples [three nulliparous (N1-N3) and three parous (P1-P3)] were clustered based solely on the expression of genes in the 70-gene parity signature. *C,* clustering analysis based solely on the expression of the 70-gene parity signature was performed on nulliparous and parous samples from Lewis, Wistar-Furth, Fischer, and Copenhagen rats. *D,* the 70-gene rat parity signature was mapped to the mouse genome using Homologene, yielding 47 mouse genes. Six FVB mouse samples [three nulliparous (N1-N3) and three parous (P1-P3)] were clustered based on the expression profiles of these 47 genes.

constituting the rat parity signature to the mouse genome, and assessed their expression profiles in nulliparous and parous FVB mouse mammary samples. Of the 70 genes that were mapped, 47 were represented on Affymetrix MGU74Av2 microarrays. These 47 genes were sufficient to distinguish nulliparous from parous samples in a blinded manner (Fig. 2*D*). Thus, a parity-related gene expression signature generated in the rat is able to predict reproductive history in the mouse, suggesting that the persistent molecular alterations that occur in response to parity are conserved across rodent species.

Among the 70 genes that we identified as being consistently regulated by parity, at least five categories were evident.

Table 1. Genes up-regulated in parous rats

Gene name	Symbol	Gene ID	Function	Category	Fold-change G1P1 versus G0P0				
					Lewis	WF	F344	Cop	Median
Immunoglobulin heavy chain	*Igha*	314487	Immunoglobulin	Immune	39.4	25.4	4.5	6.9	25.4
Casein β	*Csn2*	29173	Milk protein	Differentiation	8.0	5.2	1.9	1.5	5.2
IgM light chain		287965	Immunoglobulin	Immune	2.5	3.8	1.8	1.6	2.5
Matrix metalloproteinase 12	*Mmp12*	117033	Proteolysis	ECM/Immune	2.6	1.4	2.0	1.3	2.0
Casein γ	*Csng*	114595	Milk protein	Differentiation	3.1	1.9	1.2	0.9	1.9
Fatty acid synthase	*Fasn*	50671	Fatty acid biosynthesis	Metabolism/ differentiation	2.0	1.6	1.7	0.9	1.7
Cytochrome P450, family 4, subfamily b,1	*Cyp4b1*	24307	Monooxygenase activity	Metabolism	1.6	1.5	1.2	1.2	1.5
Carbonic anhydrase 2	*Ca2*	54231	Carbon dioxide hydration	Metabolism	1.5	1.5	1.4	1.1	1.5
Ig lambda-1 chain C region		363828	Immunoglobulin	Immune	1.5	1.4	1.4	1.3	1.4
Malic enzyme 1	*Me1*	24552	Pyruvate synthesis	Metabolism	1.3	1.4	1.4	1.1	1.4
Insulin-like growth factor binding protein 5	*Igfbp5*	25285	Igf-I-binding	Growth factor/ ECM	2.4	1.4	0.9	2.7	1.4
Lipopolysaccharide binding protein	*Lbp*	29469	Antibacterial	Immune	2.1	1.3	1.4	2.0	1.4
Polymeric immunoglobulin receptor	*Pigr*	25046	Trancytosis	Immune	1.7	1.4	1.2	1.1	1.4
Transforming growth factor, β3	*Tgfb3*	25717	Cell growth/ proliferation	Tgf-β	1.5	1.3	1.2	1.4	1.3
Aquaporin 5	*Aqp5*	25241	Water transport	Transporter	1.3	1.7	1.2	1.5	1.3
Phosphodiesterase 4B	*Pde4b*	24626	Cyclic AMP phoshodiesterase	Signal transduction	1.3	1.4	1.0	1.4	1.3
Thioesterase domain containing 1	*Thedc1*	64669	Fatty acid biosynthesis	Metabolism/ differentiation	1.9	1.2	1.3	1.5	1.3
Transferrin	*Tf*	24825	Iron transport	Transport/ differentiation	1.4	1.2	1.3	1.5	1.3
Ceruloplasmin	*Cp*	24268	Copper transport	Transport/ differentiation	1.3	1.0	1.2	2.2	1.2
Similar to death receptor 6	*Tnfrsf21*	316256	Apoptosis	Signal transduction	1.3	1.0	1.2	1.3	1.2
Aldolase C, fructose-biphosphate	*Aldoc*	24191	Fructose metabolism	Metabolism	1.2	1.2	1.1	1.3	1.2
Lipocalin 2	*Lcn2*	170496	Iron binding/antibacterial	Immune	1.3	1.1	1.2	1.4	1.2
Solute carrier family 3, member 2	*Slc3a2*	50567	Amino acid transporter	Transporter	1.2	1.1	1.2	1.3	1.2

NOTE: Genes identified as up-regulated by at least 1.2-fold in three out of four rat strains as a result of parity are reported from the highest to lowest median fold change. Gene names and symbols are reported based on the Rat Genome Database, and Gene ID according to Entrez Gene. Gene functions and categories are based on Gene Ontology.
Abbreviations: WF, Wistar-Furth; F344, Fischer 344; Cop, Copenhagen.

These included the previously identified differentiation, immune, Tgf-β, and growth factor categories (6), as well as an additional category of genes that are involved in ECM structure and function (Tables 1 and 2). We previously showed that clustering based on genes in each of the first four categories was sufficient to distinguish between nulliparous and parous rats (6). In an analogous manner, we tested whether unsupervised clustering based solely on ECM-related genes would be sufficient to differentiate between nulliparous and parous rat or mouse samples. In each case, ECM-related gene expression patterns alone were sufficient to distinguish between nulliparous and parous mammary samples from the four different rat strains (Fig. 3*A*), from independent mammary samples derived from nulliparous and parous Lewis rats (Fig. 3*B*), and from mammary samples derived from FVB mice (Fig. 3*C*). This indicates that differential expression of a subset of genes involved in ECM structure and function represents a conserved feature of parity-induced changes in the rodent mammary gland.

Parity up-regulates *Tgfb3* and expression of differentiation and immune markers. Our previous analysis of parity-induced gene expression changes in FVB mice was consistent with the parity-induced up-regulation of Tgf-β3 activity. Similarly, in the current study, we found that *Tgfb3* expression was up-regulated by parity in each of the four rat strains examined (Table 1). This finding was confirmed by QRT-PCR

Table 2. Genes down-regulated in parous rats

Gene name	Symbol	Gene ID	Function	Category	Fold-change G1P1 versus G0P0				
					Lewis	WF	F344	Cop	Median
Periostin	*Postn*	361945	Transcription factor	Differentiation	1.9	2.1	1.8	2.2	2.0
Amphiregulin	*Areg*	29183	Epidermal growth factor receptor ligand	Growth factor	3.5	2.1	1.7	1.9	2.0
Cellular retinoic acid binding protein I	*Crabp1*	25061	Retinoic acid receptor signaling	Signal transduction	1.8	2.1	1.3	1.5	1.7
Insulin-like growth factor 1	*Igf-I*	24482	Cell proliferation/ survival	Growth factor	1.7	1.2	1.5	1.5	1.5
Fibronectin 1	*Fn1*	25661	Integrin signaling	ECM	1.4	1.3	1.5	1.6	1.5
A kinase (PRKA) anchor protein (gravin) 12	*Akap12*	83425	Scaffolding protein	Signal transduction	1.2	1.6	1.6	1.3	1.4
Neuronatin	*Nnat*	94270	Protein transport		2.0	1.4	1.5	0.9	1.4
Glycosylation dependent cell adhesion molecule 1	*Glycam1*	25258	Selectin ligand	Differentiation	0.5	2.2	1.2	1.7	1.4
Secreted acidic cysteine rich glycoprotein	*Sparc*	24791	ECM Formation	ECM	1.6	1.1	1.4	1.4	1.4
Ectonucleotide pyrophosphatase/ phosphodiesterase 2	*Enpp2*	84050	Lysophospholipase	Cell motility	2.1	1.4	1.4	1.0	1.4
Lectin, galactose binding, soluble 1	*Lgals1*	56646	Integrin signaling	ECM	1.5	1.2	1.4	1.4	1.4
Inhibitor of DNA binding 1, helix-loop-helix protein	*Id1*	25261	Transcriptional repression	Tgf-β	1.4	1.4	1.4	1.1	1.4
Follistatin-like 1	*Fstl1*	79210			1.5	1.7	1.2	1.2	1.4
Phosphoserine aminotransferase 1	*Psat1*	293820	Serine biosynthesis	Metabolism	1.4	1.2	1.5	1.3	1.4
Lumican	*Lum*	81682	Proteoglycan	ECM	1.3	1.5	1.1	1.4	1.3
Melanocyte-specific gene 1 protein	*Cited1*	64466	Transcription factor	Signal transduction	1.4	1.9	1.2	1.3	1.3
Serine proteinase inhibitor, clade H, member 1	*Serpinh1*	29345	Procollagen binding	ECM	1.4	1.3	1.3	1.4	1.3
Sushi-repeat-containing protein	*Sprx*	64316			1.3	1.3	1.3	1.5	1.3
Carboxylesterase 3	*Ces3*	113902	Fatty acid metabolism	Metabolism	1.8	1.1	1.3	1.4	1.3
Cysteine rich protein 61	*Cyr61*	83476	Integrin signaling	ECM	1.1	1.3	1.3	1.6	1.3
Solute carrier family 1, member 3	*Slc1a3*	29483	Amino acid transporter	Transporter	1.4	1.3	1.3	1.1	1.3
Similar to RIKEN cDNA 6330406I15	*RDG1307396*	360757			1.6	1.2	1.3	1.3	1.3
Catalase	*Cat*	24248	Hydrogen peroxide reductase	ROS	1.7	1.0	1.4	1.2	1.3
Tropomyosin 1, α	*Tpm1*	24851	Actin binding		1.1	1.3	1.3	1.3	1.3
Activity and neurotransmitter-induced early gene protein 4	*Ania4*	360341	CAM kinase	Kinase	1.5	1.2	1.2	1.3	1.3
Solute carrier family 11, member 2	*Slc11a2*	25715	Divalent metal ion transporter	Transporter	1.4	1.0	1.3	1.2	1.3
Inhibitor of DNA binding 3, helix-loop-helix protein	*Id3*	25585	Transcriptional repression	Tgf-β	1.5	1.2	1.3	0.9	1.3
Solute carrier family 25 member 4	*Slc25a4*	85333	Nucleotide translocator	Transporter	1.3	1.3	1.2	1.3	1.3
Growth hormone receptor	*Ghr*	25235	Growth hormone signaling	Growth factor	2.1	1.1	1.2	1.3	1.3
Phosphoglycerate kinase 1	*Pgk1*	24644	Phosphoprotein glycolysis	Metabolism	1.6	1.2	1.3	1.2	1.3

(*Continued on the following page*)

Table 2. Genes down-regulated in parous rats (Cont'd)

Gene name	Symbol	Gene ID	Function	Category	Fold-change G1P1 versus G0P0				
					Lewis	WF	F344	Cop	Median
Cytosolic cysteine dioxygenase 1	*Cdo1*	81718	Cysteine metabolism	Metabolism	1.5	1.2	1.2	1.3	1.3
Mast cell protease 1	*Mcpt1*	29265	Proteolysis	ECM	1.6	1.3	1.2	1.2	1.2
Collagen, type V, α2	*Col5a2*	85250	ECM structural protein	ECM	1.0	1.2	1.3	1.5	1.2
Carbonic anhydrase 3	*Ca3*	54232	Carbon metabolism	Metabolism	1.8	1.2	1.1	1.3	1.2
Tubulin, α1	*Tuba1*	64158	Microtubule component	Cell structure	1.5	1.2	1.2	1.2	1.2
Angiotensin II receptor, type 1	*Agtr1A*	24180	Angiotensin receptor	Signal transduction	1.3	1.2	1.2	1.3	1.2
Collagen, type 1, α 1	*Col1a1*	29393	ECM structural protein	ECM	1.1	1.2	1.2	1.8	1.2
Annexin A5	*Anxa5*	25673	Calcium ion binding		1.6	1.2	1.2	1.2	1.2
Thymosin, β10	*Tmsb10*	50665	Actin binding		1.3	1.2	1.2	1.0	1.2
Tubulin, β5	*Tubb5*	29214	Microtubule component	Cell structure	1.1	1.3	1.2	1.2	1.2
Histone deacetylase 2	*Hdac2*	84577	Chromatin rearrangement		1.2	1.2	1.3	1.1	1.2
Lectin, galactose binding, soluble 7	*Lgals7*	29518	Galactose binding		1.1	1.8	1.2	1.2	1.2
CD74 antigen	*Cd74*	25599		Immune	1.2	1.2	1.0	1.3	1.2
Proteasome 26S subunit, ATPase 2	*Psmc2*	25581	Protein degradation		1.3	1.1	1.2	1.1	1.2
MORF-related gene X	*Morf412*	317413			1.4	1.2	1.1	1.2	1.2

NOTE: Genes identified as down-regulated by at least 1.2-fold in three out of four rat strains as a result of parity are reported from the highest to lowest median fold change. Gene names and symbols are reported based on the Rat Genome Database, and Gene ID according to Entrez Gene. Gene functions and categories are based on Gene Ontology.
Abbreviations: WF, Wistar-Furth; F344, Fischer 344; Cop, Copenhagen.

analysis of independent parous and nulliparous Lewis rat samples (Fig. 4*A*).

Also consistent with our prior observations, parity resulted in a persistent increase in the expression of genes involved in mammary differentiation, including the milk proteins β-casein and γ-casein, and the metal ion transporters ceruloplasmin and tranferrin (ref. 6; Table 1; Fig. 4*A*).

As we have previously shown in the mouse, the 70-gene rat parity-related gene expression signature reflected the increased presence of immune cells in the parous mammary gland. In particular, increased expression of multiple immunoglobulin heavy and light chain genes in the parous gland suggested an increase in the population of plasma cells, whereas up-regulation of *Mmp12* and *Tnfrsf21* was consistent with increased numbers of macrophages and T cells (Table 1; Fig. 4*A*). Similarly, increased antibacterial and antiviral activity was suggested by the up-regulation of *Lbp, Lcn2*, and *Ccl5* (refs. 24–26; Table 1).

Parity results in down-regulation of amphiregulin and the growth hormone/Igf-I axis. Previous gene expression profiling of mouse mammary development revealed that parity results in a persistent decrease in the expression of several growth factor–encoding genes, including *Areg* and *Igf-I* (6). The present study confirmed that decreased expression of *Areg* and *Igf-I* are consistent features of the parous state in rats (Table 2; Fig. 4*B*). Additional evidence supporting parity-induced down-regulation of the growth hormone/Igf-I axis in the mammary glands of multiple rat strains was suggested by a decrease in growth hormone receptor (*Ghr*) expression (Table 2; Fig. 4*B*) as well as an increase in *Igfbp5* expression (Table 1; Fig. 4*A*), which functions to sequester local Igf-I in the ECM (27).

Parity regulates ECM gene expression. Mammary epithelial-ECM interactions play an important role in both normal mammary gland development and tumorigenesis (28). Moreover, persistent changes in the structure and function of the ECM have been shown in the mammary glands of parous rats (29). In the present study, microarray expression profiling suggested that a principal effect of parity in the rodent mammary gland is alteration of ECM gene expression. Thirteen of the 70 genes constituting the parity signature encode ECM structural components or proteins that regulate ECM formation or signaling (Tables 1 and 2). Notably, the majority of ECM-related gene expression changes induced by parity represented decreases in expression, including the ECM structural components, fibronectin 1, lumican, and collagen type I and collagen type V (Table 2). Parity-induced decreases in the expression of genes that regulate ECM formation or cellular interactions were also observed, including, *Sparc, Lgals1, Lgals7, Serpinh1, Cyr61*, and *Mcpt1* (Table 2; Fig. 4*B*).

To determine whether these parity-induced ECM-related gene expression changes were accompanied by differences in ECM structure, we stained histologic sections with Mason's trichrome to evaluate total collagen content. Although proximal epithelial structures seemed similar with respect to periductal trichrome staining (data not shown), a significant decrease in the extent of trichrome staining surrounding distal ducts was observed in the parous gland (Fig. 4*C*). These results provide further evidence that parity results in structural changes in the ECM.

Discussion

Women who have their first child early in life have a substantially reduced lifetime risk of breast cancer, an effect that is largely restricted to ER-positive tumors. Similar to humans, rats frequently develop ER-positive breast cancers and exhibit parity-induced protection against mammary tumorigenesis. In the current study, we set out to identify persistent parity-induced changes in gene expression that are conserved among multiple rat strains that exhibit hormone-induced protection against mammary tumorigenesis. We found that four genetically diverse inbred rat strains exhibit hormone-induced protection against mammary tumorigenesis and share a 70-gene pregnancy-induced expression signature. Our findings constitute the first global survey of parity-induced changes in gene expression in the rat—which represents the principal model for studying this phenomenon—as well as the first study to show conservation of parity-induced gene expression changes in multiple inbred rat strains that exhibit hormone-induced protection. Beyond suggesting that parity-induced protection is as robust and widely conserved a phenomenon in rats as it is in humans, our findings provide new insights into potential mechanisms by which early first-full term pregnancy decreases breast cancer risk.

These current studies extend our previous observations that parity results in persistently increased mammary expression of *Tgfb3* to include multiple additional strains of rats. Notably, loss of Tgf-β signaling in stromal fibroblasts promotes the growth and invasion of mammary carcinomas (30). Tgf-β may also have direct effects on mammary epithelial cells, resulting in the inhibition of mammary tumorigenesis (31). The sum of these effects is predicted to decrease the susceptibility of the parous gland to oncogenic transformation.

One of the most consistent and robust parity-induced changes in gene expression that we have observed in the rodent mammary gland is down-regulation of the epidermal growth factor receptor ligand, *Areg*. AREG is overexpressed in a high proportion of human breast cancers and correlates with large tumor size and nodal involvement (32). Studies in genetically engineered mice and mammary epithelial cell lines suggest an important role for AREG in driving mammary epithelial proliferation, whereas recent evidence indicates that this growth factor may alter the ECM by the regulation of protease expression and secretion, including matrix metalloproteinase-2, matrix metalloproteinase-9, urokinase-type plasminogen activator, and plasminogen activator inhibitor-1 (33). Thus, parity-mediated down-regulation of *Areg* may not only inhibit epithelial proliferation, but may also hinder the invasive abilities of transformed cells in the mammary gland.

In addition to the down-regulation of *Areg*, we have confirmed that parity also results in the persistent down-regulation of *Igf-I*. Notably, a strong positive correlation exists between serum IGF-I levels and breast cancer risk in premenopausal women (34). Local and serum levels of IGF-I are regulated by growth hormone through its interaction with growth hormone receptor (35). Additional findings indicate that parity results in a persistent decrease in circulating growth hormone levels in rats (7); moreover, treatment of parous rats with Igf-I results in an increase in carcinogen-induced mammary tumorigenesis to levels similar to those observed in nulliparous controls (36). Consistent with this, spontaneous dwarf rats, which lack functional growth hormone, are highly resistant to carcinogen-induced mammary tumorigenesis (37).

Additional evidence for down-regulation of the growth hormone/Igf-I axis within the parous mammary gland was suggested in the present study by increases in *Igfbp5* expression and decreases in *Ghr* expression. As such, our findings suggest that—in addition to reducing circulating levels of growth hormone—parity may modulate local expression and activity of Igf-I within the mammary gland. Whereas Igf-I acts directly on mammary epithelial cells to promote proliferation and inhibit apoptosis (38), Igf-I in the mammary gland is likely produced in the stromal compartment in response to Ghr signaling (39). Local regulation of Igf-I activity also occurs through interactions with Igf-I binding proteins, such as Igfbp5, which binds and sequesters Igf-I in the ECM (40). As such, parity-induced down-regulation of Ghr and Igf-I expression in the mammary gland, coupled with up-regulation of Igfbp5 expression, would be predicted to result in decreased Igf-I activity. This represents a

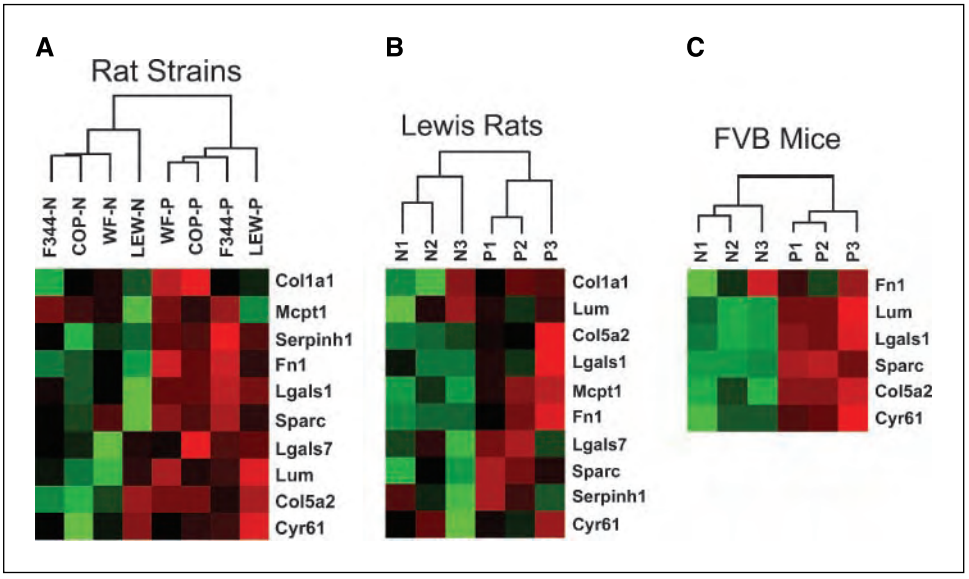

Figure 3. ECM gene expression distinguishes between nulliparous and parous rats and mice. Unsupervised hierarchical clustering analysis. *A,* a subset of parity-regulated genes involved in ECM structure and regulation was used to cluster nulliparous and parous mammary samples from Lewis (*LEW*), Wistar-Furth (*WF*), Fischer (*F344*), and Copenhagen (*COP*) rats. *B,* six independent Lewis samples [three nulliparous (N1-N3) and three parous (P1-P3) samples] were clustered based on the expression of ECM-related genes. *C,* six FVB mouse samples [three nulliparous (N1-N3) and three parous (P1-P3)] were clustered based on the expression of ECM-related genes identified in the rat parity signature that were mapped to the mouse genome.

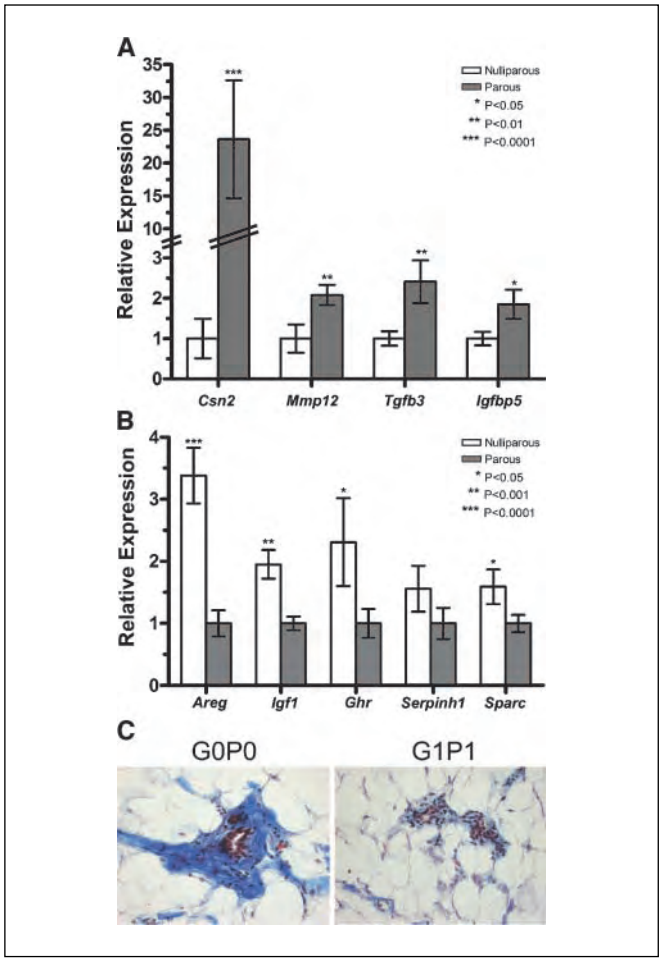

Figure 4. Confirmation of gene expression changes. *A* and *B,* TaqMan QRT-PCR was performed on cDNAs generated from 21 nulliparous and 21 parous Lewis rat mammary samples. Each reaction was performed in duplicate. Expression values for each gene were normalized to *B2m*. *A,* relative expression of parity up-regulated genes. *White columns*, mean expression in nulliparous samples normalized to 1.0 for each gene; *gray columns*, mean expression of each gene in parous relative to nulliparous samples; *bars*, ±SE. *B,* relative expression of parity down-regulated genes. *White columns*, mean expression of each gene in nulliparous relative to parous samples; *gray columns,* mean expression in parous samples normalized to 1.0 for each gene; *bars*, ±SE. *P* values were generated using a one-tailed, unpaired Student's *t* test. *C,* Mason's trichrome staining. Abdominal mammary glands from nulliparous and parous Lewis rats were stained with Mason's trichrome to assess total collagen present in the ECM surrounding epithelial structures. Images are representative of distal structures in the mammary glands of three nulliparous and three parous Lewis rats (original magnification, ×200).

plausible mechanism by which parity may confer protection against breast cancer.

The functional unit of the mammary gland consists of a complex stroma that surrounds the epithelial compartment. Stromal-epithelial interactions play a prominent role, not only in mammary development, but also in tumorigenesis (28). Fibroblasts represent the most prominent cell type of the periductal stroma and, in addition to secreting growth factors that activate epithelial receptors, they are the primary synthesizers of ECM constituents such as fibronectin, collagen, and proteoglycans. Accumulating evidence indicates that stromal constituents, including fibroblasts and ECM structural components, could have differential effects on epithelial cells depending on the source of the tissue from which they are isolated (41). Consistent with this, Schedin et al. have shown that the ability of mammary epithelial cells to form ductal structures in culture is markedly influenced by the developmental context of the ECM in which they are cultured (29). Further support for the role of ECM regulation in parity-induced protection against breast cancer comes from our observation that parous mammary glands exhibit decreased trichrome staining as well as persistent down-regulation of ECM structural and regulatory genes. Because cross-talk between epithelial and stroma cells occurs through local growth factors and their receptors (42), it is possible that parity-induced down-regulation of *Areg* and *Igf-I* in combination with up-regulation of *Tgfb3* may alter stromal-epithelial interactions in such a way as to decrease susceptibility to mammary carcinogenesis.

Finally, it is interesting to speculate that parity-induced changes in the ECM may be related to measures of breast cancer risk associated with mammographic breast density. Increased mammographic density has been consistently shown to correlate with high breast cancer risk (43). Mammographic density has also been reported to be negatively correlated with parity (44). Although breast density was initially believed to reflect the epithelial content of the breast, current evidence suggests that ECM composition—in particular collagen and proteoglycans such as lumican—may be the primary determinant of mammographic density (44, 45). Intriguingly, recent studies have implicated the ratio of serum IGF-I to IGFBP3 as a major determinant of mammographic density (46). Consistent with this, Guo et al. found increased IGF-I tissue staining in samples from women with increased breast density (45). Our findings support the hypothesis that parity decreases Igf-I expression and activity and diminishes the expression of selected ECM structural components. Together, these changes may lead to decreases in both mammographic breast density and breast cancer risk. Validation of this hypothesis will require confirmation that parity alters local IGF-I levels and mammographic breast density in women, and that modulation of Igf-I in rodent models will alter breast density as well as pregnancy-induced protection against breast cancer.

In summary, the results presented in this study extend previous observations that parity results in local changes in growth factor gene expression in the mammary gland. We hypothesize that the evolutionarily conserved parity-induced alterations in gene expression identified in this study result in the modification of the extracellular environment and changes in stromal-epithelial interactions. We hypothesize that the ultimate effect of these changes is to create a tumor suppressive state, thereby providing a potential mechanism to explain parity-induced protection against mammary tumorigenesis. Whether analogous parity-induced changes occur in the human breast remains an important yet unresolved question.

Acknowledgments

Received 11/29/2005; revised 3/28/2006; accepted 4/24/2006.

Grant support: CA92910 from the National Cancer Institute, grants W81XWH-05-1-0405, W81XWH-05-1-0390, DAMD17-03-1-0345 (C.M. Blakely), and DAMD17-00-1-0401 (S.E. Moody) from the U.S. Army Breast Cancer Research Program, and grants from the Breast Cancer Research Foundation and the Emerald Foundation.

The costs of publication of this article were defrayed in part by the payment of page charges. This article must therefore be hereby marked *advertisement* in accordance with 18 U.S.C. Section 1734 solely to indicate this fact.

The authors thank the members of the Chodosh Laboratory for helpful discussions and critical reading of the manuscript.

References

1. Chodosh LA, D'Cruz CM, Gardner HP, et al. Mammary gland development, reproductive history, and breast cancer risk. Cancer Res 1999;59:1765–71.
2. MacMahon B, Cole P, Lin TM, et al. Age at first birth and breast cancer risk. Bull World Health Organ 1970;43: 209–21.
3. Layde PM, Webster LA, Baughman AL, Wingo PA, Rubin GL, Ory HW. The independent associations of parity, age at first full term pregnancy, and duration of breastfeeding with the risk of breast cancer. Cancer and Steroid Hormone Study Group. J Clin Epidemiol 1989;42: 963–73.
4. Russo J, Moral R, Balogh GA, Mailo D, Russo IH. The protective role of pregnancy in breast cancer. Breast Cancer Res 2005;7:131–42.
5. Sivaraman L, Medina D. Hormone-induced protection against breast cancer. J Mammary Gland Biol Neoplasia 2002;7:77–92.
6. D'Cruz CM, Moody SE, Master SR, et al. Persistent parity-induced changes in growth factors, TGF-β3, and differentiation in the rodent mammary gland. Mol Endocrinol 2002;16:2034–51.
7. Thordarson G, Jin E, Guzman RC, Swanson SM, Nandi S, Talamantes F. Refractoriness to mammary tumorigenesis in parous rats: is it caused by persistent changes in the hormonal environment or permanent biochemical alterations in the mammary epithelia? Carcinogenesis 1995;16:2847–53.
8. Russo J, Gusterson BA, Rogers AE, Russo IH, Wellings SR, van Zwieten MJ. Comparative study of human and rat mammary tumorigenesis. Lab Invest 1990;62:244–78.
9. Sivaraman L, Stephens LC, Markaverich BM, et al. Hormone-induced refractoriness to mammary carcinogenesis in Wistar-Furth rats. Carcinogenesis 1998;19: 1573–81.
10. Yang J, Yoshizawa K, Nandi S, Tsubura A. Protective effects of pregnancy and lactation against *N*-methyl-*N*-nitrosourea-induced mammary carcinomas in female Lewis rats. Carcinogenesis 1999;20:623–8.
11. Rajkumar L, Guzman RC, Yang J, Thordarson G, Talamantes F, Nandi S. Short-term exposure to pregnancy levels of estrogen prevents mammary carcinogenesis. Proc Natl Acad Sci U S A 2001;98:11755–9.
12. Guzman RC, Yang J, Rajkumar L, Thordarson G, Chen X, Nandi S. Hormonal prevention of breast cancer: mimicking the protective effect of pregnancy. Proc Natl Acad Sci U S A 1999;96:2520–5.
13. Medina D, Smith GH. Chemical carcinogen-induced tumorigenesis in parous, involuted mouse mammary glands. J Natl Cancer Inst 1999;91:967–69.
14. Medina D, Kittrell FS. p53 function is required for hormone-mediated protection of mouse mammary tumorigenesis. Cancer Res 2003;63:6140–3.
15. Ginger MR, Gonzalez-Rimbau MF, Gay JP, Rosen JM. Persistent changes in gene expression induced by estrogen and progesterone in the rat mammary gland. Mol Endocrinol 2001;15:1993–2009.
16. Colditz GA, Rosner BA, Chen WY, Holmes MD, Hankinson SE. Risk factors for breast cancer according to estrogen and progesterone receptor status. J Natl Cancer Inst 2004;96:218–28.
17. Turcot-Lemay L, Kelly PA. Response to ovariectomy of *N*-methyl-*N*-nitrosourea-induced mammary tumors in the rat. J Natl Cancer Inst 1981;66:97–102.
18. Master SR, Stoddard AJ, Bailey LC, Pan TC, Dugan KD, Chodosh LA. Genomic analysis of early murine mammary gland development using novel probe-level algorithms. Genome Biol 2005;6:R20.
19. Gentleman RC, Carey VJ, Bates DM, et al. Bioconductor: open software development for computational biology and bioinformatics. Genome Biol 2004;5:R80.
20. Phang TL, Neville MC, Rudolph M, Hunter L. Trajectory clustering: a non-parametric method for grouping gene expression time courses, with applications to mammary development. Pac Symp Biocomput 2003;351–62.
21. Waha A, Sturne C, Kessler A, et al. Expression of the ATM gene is significantly reduced in sporadic breast carcinomas. Int J Cancer 1998;78:306–9.
22. Ito K, Fujimori M, Nakata S, et al. Clinical significance of the increased multidrug resistance-associated protein (MRP) gene expression in patients with primary breast cancer. Oncol Res 1998;10:99–109.
23. Gould MN, Zhang R. Genetic regulation of mammary carcinogenesis in the rat by susceptibility and suppressor genes. Environ Health Perspect 1991;93:161–7.
24. Flo TH, Smith KD, Sato S, et al. Lipocalin 2 mediates an innate immune response to bacterial infection by sequestrating iron. Nature 2004;432:917–21.
25. Elliott MB, Tebbey PW, Pryharski KS, Scheuer CA, Laughlin TS, Hancock GE. Inhibition of respiratory syncytial virus infection with the CC chemokine RANTES (CCL5). J Med Virol 2004;73:300–8.
26. Branger J, Florquin S, Knapp S, et al. LPS-binding protein-deficient mice have an impaired defense against Gram-negative but not Gram-positive pneumonia. Int Immunol 2004;16:1605–11.
27. Flint DJ, Beattie J, Allan GJ. Modulation of the actions of IGFs by IGFBP-5 in the mammary gland. Horm Metab Res 2003;35:809–15.
28. Tlsty TD, Hein PW. Know thy neighbor: stromal cells can contribute oncogenic signals. Curr Opin Genet Dev 2001;11:54–9.
29. Schedin P, Mitrenga T, McDaniel S, Kaeck M. Mammary ECM composition and function are altered by reproductive state. Mol Carcinog 2004;41:207–20.
30. Cheng N, Bhowmick NA, Chytil A, et al. Loss of TGF-β type II receptor in fibroblasts promotes mammary carcinoma growth and invasion through upregulation of TGF-α-, MSP- and HGF-mediated signaling networks. Oncogene 2005;24:5053–68.
31. Pierce DF, Jr., Gorska AE, Chytil A, et al. Mammary tumor suppression by transforming growth factor β1 transgene expression. Proc Natl Acad Sci U S A 1995;92: 4254–8.
32. Ma L, de Roquancourt A, Bertheau P, et al. Expression of amphiregulin and epidermal growth factor receptor in human breast cancer: analysis of autocriny and stromal-epithelial interactions. J Pathol 2001;194:413–9.
33. Menashi S, Serova M, Ma L, Vignot S, Mourah S, Calvo F. Regulation of extracellular matrix metalloproteinase inducer and matrix metalloproteinase expression by amphiregulin in transformed human breast epithelial cells. Cancer Res 2003;63:7575–80.
34. Schernhammer ES, Holly JM, Pollak MN, Hankinson SE. Circulating levels of insulin-like growth factors, their binding proteins, and breast cancer risk. Cancer Epidemiol Biomarkers Prev 2005;14:699–704.
35. Laban C, Bustin SA, Jenkins PJ. The GH-IGF-I axis and breast cancer. Trends Endocrinol Metab 2003;14:28–34.
36. Thordarson G, Slusher N, Leong H, et al. Insulin-like growth factor (IGF)-I obliterates the pregnancy-associated protection against mammary carcinogenesis in rats: evidence that IGF-I enhances cancer progression through estrogen receptor-α activation via the mitogen-activated protein kinase pathway. Breast Cancer Res 2004;6:R423–36.
37. Thordarson G, Semaan S, Low C, et al. Mammary tumorigenesis in growth hormone deficient spontaneous dwarf rats; effects of hormonal treatments. Breast Cancer Res Treat 2004;87:277–90.
38. Hadsell DL, Bonnette SG. IGF and insulin action in the mammary gland: lessons from transgenic and knockout models. J Mammary Gland Biol Neoplasia 2000;5:19–30.
39. Gallego MI, Binart N, Robinson GW, et al. Prolactin, growth hormone, and epidermal growth factor activate Stat5 in different compartments of mammary tissue and exert different and overlapping developmental effects. Dev Biol 2001;229:163–75.
40. Marshman E, Green KA, Flint DJ, White A, Streuli CH, Westwood M. Insulin-like growth factor binding protein 5 and apoptosis in mammary epithelial cells. J Cell Sci 2003;116:675–82.
41. Barcellos-Hoff MH, Ravani SA. Irradiated mammary gland stroma promotes the expression of tumorigenic potential by unirradiated epithelial cells. Cancer Res 2000;60:1254–60.
42. Bhowmick NA, Neilson EG, Moses HL. Stromal fibroblasts in cancer initiation and progression. Nature 2004;432:332–7.
43. Tice JA, Cummings SR, Ziv E, Kerlikowske K. Mammographic breast density and the Gail model for breast cancer risk prediction in a screening population. Breast Cancer Res Treat 2005;94:115–22.
44. Li T, Sun L, Miller N, et al. The association of measured breast tissue characteristics with mammographic density and other risk factors for breast cancer. Cancer Epidemiol Biomarkers Prev 2005;14:343–9.
45. Guo YP, Martin LJ, Hanna W, et al. Growth factors and stromal matrix proteins associated with mammographic densities. Cancer Epidemiol Biomarkers Prev 2001;10:243–8.
46. Diorio C, Pollak M, Byrne C, et al. Insulin-like growth factor-I, IGF-binding protein-3, and mammographic breast density. Cancer Epidemiol Biomarkers Prev 2005;14:1065–73.

Correction: Pregnancy-Induced Protection against Mammary Tumorigenesis

In the article on pregnancy-induced protection against mammary tumorigenesis in the June 15, 2006 issue of *Cancer Research* (1), the parity status of six of the 43 arrays used to derive the 70-gene expression signature was misclassified through an error in data entry. These arrays represented six of the 14 arrays run for Fischer 344 rats. The remaining 37 arrays for the Lewis, Wistar-Furth, Copenhagen, and Fischer 344 mammary samples were properly classified, as were the independent Lewis rat and FVB mouse samples used to validate the findings. This misclassification both obscured genuine parity-induced changes in the Fischer 344 strain and added biological noise due to genes that were covarying but unrelated to parity. As a consequence, after correcting the parity status for the six Fischer 344 arrays and applying the same analytical criteria described in the article, the authors found that the core parity-induced gene expression signature was reduced from 70 to 47 genes. Similar to the original 70-gene signature, this 47-gene signature is sufficient to distinguish between independent nulliparous and parous samples from all rat and mouse strains analyzed in the article. Corrected versions of Tables 1 and 2 appear below.

Each of the five originally identified functional gene categories (Tgf-β3, differentiation, immune markers, growth hormone/Igf-1 axis, and extracellular matrix components) are retained within this signature. Genes lost from the original 70-gene signature remain significantly altered in two of the four rat strains and are still plausible candidates for contributing to parity-induced protection against mammary tumorigenesis. Notably, a role for downregulation of *Ghr*, which is not included in the corrected signature, in parity-induced protection is still supported by the FVB mouse data and the QRT-PCR analysis of independent Lewis rat samples presented in the article. Also consistent with a role for the GH/Igf-1 pathway in parity-induced protection, *Igf-1* remains downregulated — and *Igfbp5* remains upregulated — on the corrected list of genes.

Overall, despite the reassignment of six samples, the conclusions of the article remain unaltered. Moreover, as a primary goal of the original article was to narrow down the list of genes to those most robustly associated with parity-induced protection, the corrected signature accomplishes this and provides an even

Table 1. Genes up-regulated in parous rats

Gene name	Symbol	Gene ID	Function	Category	Fold-change G1P1 versus G0P0				
					Lewis	WF	F344	Cop	Median
Immunoglobulin heavy chain	*Igha*	314487	Immunoglobulin	Immune	39.4	25.4	12.4	6.9	18.9
Casein beta	*Csn2*	29173	Milk protein	Differentiation	8.0	5.2	1.6	1.5	3.4
IgM light chain		287965	Immunoglobulin	Immune	2.5	3.8	2.0	1.6	2.2
Insulin-like growth factor binding protein 5	*Igfbp5*	25285	Igf1-binding	Growth factor/ ECM	2.4	1.4	1.1	2.7	1.9
Casein gamma	*Csng*	114595	Milk protein	Differentiation	3.1	1.9	1.8	0.9	1.9
Lipopolysaccharide binding protein	*Lbp*	29469	Antibacterial	Immune	2.1	1.3	1.0	2.0	1.7
Matrix metalloproteinase 12	*Mmp12*	117033	Proteolysis	ECM/Immune	2.6	1.4	1.6	1.3	1.5
Carbonic anhydrase 2	*Ca2*	54231	Carbon metabolism	Metabolism	1.5	1.5	1.5	1.1	1.5
Fatty acid synthase	*Fasn*	50671	Fatty acid biosynthesis	Metabolism/ Differentation	2.0	1.6	1.3	0.9	1.5
Cytochrome P450, family 4, subfamily b,1	*Cyp4b1*	24307	Monooxygenase activity	Metabolism	1.6	1.5	1.4	1.2	1.4
Transforming growth factor, beta 3	*Tgfb3*	25717	Cell growth/ proliferation	Tgf-β	1.5	1.3	0.9	1.4	1.4
Thioesterase domain containing 1	*Thedc1*	64669	Fatty acid biosynthesis	Metabolism/ Differentation	1.9	1.2	0.8	1.5	1.3
Malic enzyme 1	*Me1*	24552	Pyruvate synthesis	Metabolism	1.3	1.4	1.4	1.1	1.3
Phosphodiesterase 4B	*Pde4b*	24626	cAMP phoshodiesterase	Signal transduction	1.3	1.4	0.8	1.4	1.3
Polymeric immunoglobulin receptor	*Pigr*	25046	Trancytosis	Immune	1.7	1.4	1.2	1.1	1.3
Kruppel-like factor 9	*Klf9*	117560	Transcription Factor	Signal transduction	1.3	1.4	1.2	1.1	1.3
Matrix metalloproteinase 11	*Mmp11*	25481	Proteolysis	ECM	1.2	1.2	1.2	1.2	1.2

NOTE: Genes identified as up-regulated by at least 1.2-fold in three out of four rat strains as a result of parity are reported from highest to lowest median fold-change. Gene names and symbols are reported based on the Rat Genome Database, and Gene ID according to Entrez Gene. Gene functions and categories are based upon GeneOntology.
Abbreviations: WF, Wistar-Furth; F344, Fischer 344; Cop, Copenhagen.

doi:10.1158/0008-5472.CAN-67-2-COR2

smaller overlap of evolutionarily conserved gene expression changes associated with parity-induced protection against mammary tumorigenesis.

1. Blakely CM, Stoddard AJ, Belka GK, Dugan KD, Notarfrancesco KL, Moody SE, D'Cruz CM, Chodosh LA. Hormone-induced protection against mammary tumorigenesis is conserved in multiple rat strains and identifies a core gene expression signature induced by pregnancy. Cancer Res 2006;66:6421–31.

Table 2. Genes down-regulated in parous rats

Gene name	Symbol	Gene ID	Function	Category	Fold-change G0P0 versus G1P1				
					Lewis	WF	F344	Cop	Median
Periostin	*Postn*	361945	Cell adhesion	ECM	1.9	2.1	1.6	2.2	2.0
Amphiregulin	*Areg*	29183	Epidermal growth factor receptor ligand	Growth factor	3.5	2.1	1.9	1.9	2.0
Cellular retinoic acid binding protein I	*Crabp1*	25061	Retinoic acid receptor signaling	Signal transduction	1.8	2.1	1.3	1.5	1.7
Glycosylation dependent cell adhesion molecule 1	*Glycam1*	25258	Selectin ligand	Differentiation	0.5	2.2	1.3	1.7	1.5
Secreted acidic cysteine rich glycoprotein	*Sparc*	24791	ECM Formation	ECM	1.9	1.3	1.1	1.7	1.5
Lumican	*Lum*	81682	Proteoglycan	ECM	1.3	1.5	1.5	1.4	1.5
3-hydroxy-3-methylglutaryl-Coenzyme A synthase 2	*Hmgcs2*	24450	Cholesterol/ketone body biosynthesis	Metabolism	2.9	1.3	1.6	1.0	1.5
Fibronectin 1	*Fn1*	25661	Integrin signaling	ECM	1.4	1.3	1.3	1.6	1.4
Cbp/p300-interacting transactivator with Glu/Asp-rich carboxy-terminal domain 1	*Cited1*	64466	Transcription factor	Signal transduction	1.4	1.9	1.3	1.3	1.4
Ectonucleotide pyrophosphatase/phosphodiesterase 2	*Enpp2*	84050	Lysophospholipase	Cell motility	1.7	1.4	0.8	1.3	1.4
Insulin-like growth factor 1	*Igf1*	24482	Cell proliferation/survival	Growth factor	1.7	1.2	1.1	1.5	1.3
Sushi-repeat-containing protein	*Sprx*	64316			1.3	1.3	1.1	1.5	1.3
Lectin, galactose binding, soluble 1	*Lgals1*	56646	Integrin signaling	ECM	1.5	1.2	0.8	1.4	1.3
A kinase (PRKA) anchor protein (gravin) 12	*Akap12*	83425	Scaffolding protein	Signal transduction	1.2	1.6	1.2	1.3	1.3
Lectin, galactose binding, soluble 7	*Lgals7*	29518	Galactose binding		1.1	1.8	1.4	1.2	1.3
Tropomyosin 1, alpha	*Tpm1*	24851	Actin binding		1.1	1.3	1.3	1.3	1.3
Activity and neurotransmitter induced early gene protein 4	*Ania4*	360341	CAM kinase	Kinase	1.5	1.2	1.0	1.3	1.3
Cytosolic cysteine dioxygenase 1	*Cdo1*	81718	Cysteine metabolism	Metabolism	1.5	1.2	0.8	1.3	1.3
Carbonic anhydrase 3	*Ca3*	54232	Carbon metabolism	Metabolism	1.8	1.2	0.8	1.3	1.2
CD74 antigen	*Cd74*	25599		Immune	1.2	1.2	1.3	1.3	1.2
Tubulin, alpha 1	*Tuba1*	64158	Microtubule component	Cell structure	1.5	1.2	0.9	1.2	1.2
Similar to RIKEN cDNA 6330406I15	*RGD1307396*	360757			1.6	1.2	1.0	1.3	1.2
Collagen, type 1, alpha 1	*Col1a1*	29393	ECM structural protein	ECM	0.9	1.2	1.2	1.6	1.2
Phosphoglycerate kinase 1	*Pgk1*	24644	Phosphoprotein glycolysis	Metabolism	1.6	1.2	0.9	1.2	1.2
Annexin A5	*Anxa5*	25673	Calcium ion binding		1.6	1.2	0.8	1.2	1.2
Prohibitin	*Phb*	25344	Regulation of cell cycle	Signal transduction	1.3	1.2	1.2	1.1	1.2
Valosin-containing protein	*Vcp*	116643	Endoplasmic reticulum protein catabolism		1.2	1.2	1.2	1.2	1.2
Tropomyosin 4	*Tpm4*	24852	Actin binding		1.1	1.3	1.2	1.2	1.2
Tubulin, beta 5	*Tubb5*	29214	Microtubule component	Cell structure	1.1	1.3	1.2	1.2	1.2
MORF-related gene X	*Morf412*	317413			1.4	1.2	1.0	1.2	1.2

NOTE: Genes identified as down-regulated by at least 1.2-fold in three out of four rat strains as a result of parity are reported from highest to lowest median fold-change. Gene names and symbols are reported based on the Rat Genome Database, and Gene ID according to Entrez Gene. Gene functions and categories are based upon GeneOntology.
Abbreviations: WF, Wistar-Furth; F344, Fischer 344; Cop, Copenhagen.

Research article

Open Access

Dense breast stromal tissue shows greatly increased concentration of breast epithelium but no increase in its proliferative activity

Debra Hawes[1], Susan Downey[2], Celeste Leigh Pearce[3], Sue Bartow[4], Peggy Wan[3], Malcolm C Pike[3] and Anna H Wu[3]

[1]Department of Pathology, Keck School of Medicine, University of Southern California, 2011 Zonal Avenue, Los Angeles, CA 90089, USA
[2]Department of Surgery, Keck School of Medicine, University of Southern California, 1510 San Pablo Street, Los Angeles, CA 90033, USA
[3]Department of Preventive Medicine, Keck School of Medicine, University of Southern California/Norris Comprehensive Cancer Center, 1441 Eastlake Avenue, Los Angeles, CA 90033, USA
[4]107 Stark Mesa, Carbondale, CO 81623, USA

Corresponding author: Malcolm C Pike, mcpike@usc.edu

Received: 2 Feb 2006 Revisions requested: 21 Feb 2006 Revisions received: 8 Mar 2006 Accepted: 30 Mar 2006 Published: 28 Apr 2006

Breast Cancer Research 2006, **8**:R24 (doi:10.1186/bcr1408)
This article is online at: http://breast-cancer-research.com/content/8/2/R24

Abstract

Introduction Increased mammographic density is a strong risk factor for breast cancer. The reasons for this are not clear; two obvious possibilities are increased epithelial cell proliferation in mammographically dense areas and increased breast epithelium in women with mammographically dense breasts. We addressed this question by studying the number of epithelial cells in terminal duct lobular units (TDLUs) and in ducts, and their proliferation rates, as they related to local breast densities defined histologically within individual women.

Method We studied deep breast tissue away from subcutaneous fat obtained from 12 healthy women undergoing reduction mammoplasty. A slide from each specimen was stained with the cell-proliferation marker MIB1. Each slide was divided into (sets of) areas of low, medium and high density of connective tissue (CT; highly correlated with mammographic densities). Within each of the areas, the numbers of epithelial cells in TDLUs and ducts, and the numbers MIB1 positive, were counted.

Results The relative concentration (RC) of epithelial cells in high compared with low CT density areas was 12.3 (95% confidence interval (CI) 10.9 to 13.8) in TDLUs and 34.1 (95% CI 26.9 to 43.2) in ducts. There was a much smaller difference between medium and low CT density areas: RC = 1.4 (95% CI 1.2 to 1.6) in TDLUs and 1.9 (95% CI 1.5 to 2.3) in ducts. The relative mitotic rate (RMR; MIB1 positive) of epithelial cells in high compared with low CT density areas was 0.59 (95% CI 0.53 to 0.66) in TDLUs and 0.65 (95% CI 0.53 to 0.79) in ducts; the figures for the comparison of medium with low CT density areas were 0.58 (95% CI 0.48 to 0.70) in TDLUs and 0.66 (95% CI 0.44 to 0.97) in ducts.

Conclusion Breast epithelial cells are overwhelmingly concentrated in high CT density areas. Their proliferation rate in areas of high and medium CT density is lower than that in low CT density areas. The increased breast cancer risk associated with increased mammographic densities may simply be a reflection of increased epithelial cell numbers. Why epithelium is concentrated in high CT density areas remains to be explained.

Introduction

On a mammogram, fat appears radiolucent or dark, whereas stromal and epithelial tissue appears radio-dense or white. The amount of mammographic density is a strong independent predictor of breast cancer risk [1,2]. The biological basis for this increased risk is poorly understood. A critical question is whether densities are directly related to risk or are simply a marker of risk. We addressed this question recently by studying the location of small ductal carcinoma *in situ* (DCIS) lesions as revealed by microcalcifications, and showed that such DCIS occurs overwhelmingly in the mammographically dense areas of the breast [3]. Most DCIS lesions in our study

a_H, a_L, a_M = the areas of the slide classified as being of high, low and medium CT density (in μm^2); CI = confidence interval; CT = connective tissue; DAB = 3,3'-diaminobenzidine tetrahydrochloride; DCIS = ductal carcinoma *in situ*; n_H, n_L, n_M = the numbers of epithelial cells staining positive for MIB1 within high, low and medium CT density areas; RC = relative concentration; RMR = relative mitotic rate; TDLU = terminal duct lobular unit; t_H, t_L, t_M = the numbers of epithelial cells within high, low and medium CT density areas;

Table 1

Relation between relative concentration of epithelial cells and connective tissue density

CT density	RC	95% CI	*p*
TDLUs			
Low	1.0		
Medium	1.4	1.2–1.6	<0.001
High	12.3	10.9–13.8	<0.001
Ducts			
Low	1.0		
Medium	1.9	1.5–2.3	<0.001
High	34.1	26.9–43.2	<0.001

CI, confidence interval; CT, connective tissue; RC, relative concentration (per unit area); TDLUs, terminal duct lobular units.

occurred in the lateral-superior quadrant, as has been found in previous studies [4], and 'correlated strongly with the average percentage density in the different mammographic quadrants' [3]. Pre-DCIS mammograms that were taken on average about two years previously showed that the areas subsequently exhibiting DCIS were clearly dense at the time of the earlier mammogram, and this suggests that this relationship was not brought about by the presence of the DCIS. The reasons for these findings are not clear; two obvious possibilities are increased epithelial cell proliferation in mammographically dense areas of the breast and increased breast epithelium in women with mammographically dense breasts. Two groups have investigated the relationship between the amount of mammographic density of a woman and the amount of her breast epithelial tissue [5,6]. Alowami and colleagues [5] used tissue obtained from biopsies investigating breast lesions that were subsequently diagnosed as benign or pre-invasive breast disease; they studied tissue 'distant from the diagnostic lesion' without reference to its location as regards mammographic density (that is, 'random' tissue). They found that the median density of duct lobular units was 28% higher in breasts whose overall mammographic density was 50% or more ($n = 27$) than in breasts whose overall mammographic density was less than 25% ($n = 35$); this result was not statistically significant and the result was described as showing 'no difference in the density of epithelial components' [5]. Li and colleagues [6] also found in their much larger study ($n = 236$) of 'random' breast tissue collected from normal women by Bartow and colleagues [7] in their autopsy study of accidental deaths in New Mexico that women with high mammographic density had greater amounts of epithelial tissue (as measured by area of epithelial nuclear staining) and the result was highly statistically significant. Breast epithelial proliferation rates as they relate to mammographic densities in healthy women have not been well studied [8]. We have addressed these questions by studying the number of epithelial cells in terminal duct lobular units (TDLUs) and in breast ducts, and their respective proliferation rates as they relate to local histological breast densities within individual women.

Materials and methods

We retrospectively identified 15 consecutive healthy women who had undergone a reduction mammoplasty performed by one of us (SD) at the University of Southern California medical facilities. The study protocol was approved by the Institutional Review Board of the University of Southern California School of Medicine.

For each participant we obtained the formalin-fixed paraffin-embedded block of tissue that had been routinely processed and saved from her surgery. A single slide was cut from each block and stained with the proliferation marker MIB1 (BioGenex Laboratories, San Ramon, CA, USA). The slides were prepared in accordance with our previously published protocol [9]; the chromogen used was 3,3'-diaminobenzidine tetrahydrochloride (DAB). On microscopic examination one of the slides contained skin and two other slides showed areas of disintegration; all three were deemed unsuitable for study.

Each of the remaining 12 slides was divided into (sets of) areas of low, medium and high density of connective tissue (CT) (highly correlated with densities as defined by mammographic criteria [10]); see Figure 1. The total size of each of the three areas (in μm^2), and within each of the three areas the numbers of epithelial cells in TDLUs and ducts and the numbers that were MIB1 positive, were counted with the help of an automated microscope system that digitized the images and permitted the outlining of relevant areas on a high-resolution computer screen (ACIS II; Clarient, Inc., San Juan Capistrano, CA, USA). The total numbers of epithelial cells in different outlined areas within the CT density-defined areas was then automatically counted by the ACIS II nuclear counting software program, which is based on color identification. Hematoxylin was used to counterstain the MIB1-negative nuclei blue, and the DAB chromogen marked the MIB1-positive nuclei brown.

Figure 1

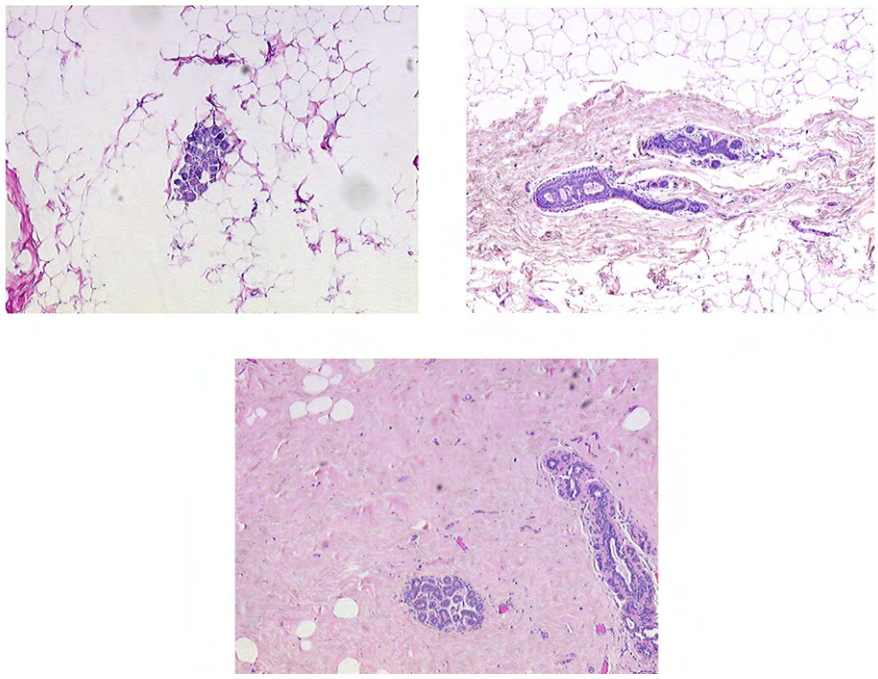

Example of areas of low, medium (upper right) and high (lower center) CT density.

The software calculated the numbers of MIB1-negative and MIB1-positive cells on the basis of these color differences.

Statistical analysis

For each slide, and separately for TDLU and ductal cells, three sets of values were obtained: first, the areas of the slide classified as being of low, medium or high CT density (a_L, a_M and a_H in μm^2); second, the numbers of epithelial cells within these areas (t_L, t_M and t_H); and third, the numbers of these epithelial cells staining positive for MIB1 (n_L, n_M and n_H). On the null hypothesis of no association between the *t*'s and the *a*'s – that is, no association between the numbers of epithelial cells and the CT density of the local tissue – the expected value of the *t*'s is simply proportional to the related *a*'s, so that, for example, the expected value of t_H is $(t_L + t_M + t_H) \times a_H/(a_L + a_M + a_H)$. Similarly, on the null hypothesis of no association between MIB1 positivity as a proportion of epithelial cells and the CT density of the local tissue, the expected value of the *n*'s is simply proportional to the related *t*'s, so that, for example, the expected value of n_H is $(n_L + n_M + n_H) \times t_H/(t_L + t_M + t_H)$. We analyzed these data with standard statistical software as implemented in the STATA statistical software package (procedure cs; Stata Corporation, Austin, TX, USA); the ratios of epithelial concentration (cells per unit area) and the ratios of proportions of epithelial cells staining positive for MIB1 are the measures of effect. All statistical significance levels (*p* values) quoted are two-sided.

Results

The 12 subjects included in the analysis were aged 18 to 60 years with a median age of 33 years; only one subject was aged 50 years or older.

Areas of the slides of low CT density comprised on average 44% of the total of areas of low plus medium plus high CT density ($a_L/(a_L + a_M + a_H)$), whereas areas of high CT density comprised on average 35% of the total area ($a_H/(a_L + a_M + a_H)$).

Table 1 shows the summary relative concentrations (RCs; ratios of cells per unit area) of epithelial cells in the three areas defined by CT density separately for TDLU cells and for ductal cells. The concentration of TDLU epithelial cells is slightly greater in the areas of medium CT density than in the areas of low CT density (RC = 1.4, 95% confidence interval (CI) 1.2 to 1.6; $p < 0.001$) but is much greater in the areas of high CT density (RC = 12.3, 95% CI 10.8 to 13.8; $p < 0.001$). The TDLU results for the individual slides (women) comparing areas of high CT density with areas of low CT density are shown in Figure 2. Although the results from individual subjects do differ somewhat, the RCs were not correlated with age (the only variable available on these women) and the summary RC seems to be a fair representation of the overall results. The results for ducts were similar.

Table 2 shows the summary relative mitotic rates (RMRs) of epithelial cells staining MIB1 positive in the three areas defined by CT density separately for TDLU cells and for ductal

Table 2

Relation between relative mitotic rate (MIB1 positive) of epithelial cells and connective tissue density

CT density	RMR	95% CI	*p*
TDLUs			
Low	1.00		
Medium	0.58	0.48–0.70	<0.001
High	0.59	0.53–0.66	<0.001
Ducts			
Low	1.00		
Medium	0.66	0.44–0.97	0.035
High	0.65	0.53–0.79	<0.001

CI, confidence interval; CT, connective tissue; RMR, relative mitotic rate; TDLUs, terminal duct lobular units.

Figure 2

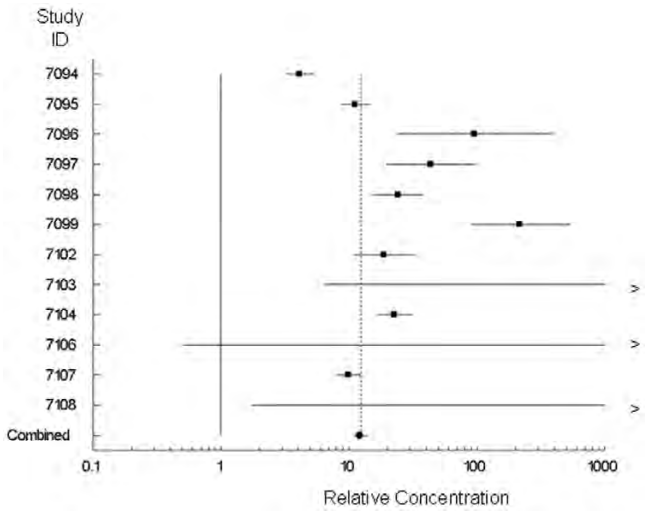

RCs (with 95% CIs) of TDLU epithelial cells in high and low CT areas.

Figure 3

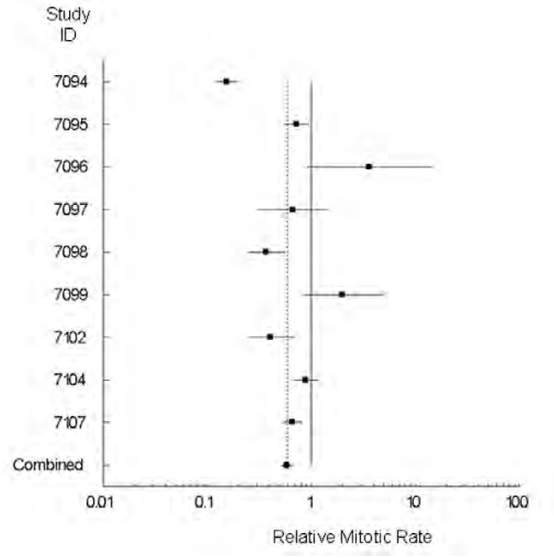

RMRs (with 95% CIs) of TDLU epithelial cells in high and low CT areas.

cells. The proportion of TDLU epithelial cells staining MIB1 positive is statistically significantly less (RMR ≈ 0.6) both in the areas of medium CT density ($p < 0.001$) and in the areas of high CT density ($p < 0.001$) than in the areas of low CT density. The median MIB1-positive proportion was about 4%. Almost all the women in this study were premenopausal on the basis of their age; this figure is close to the Ki67 figure of 4.5% given for healthy premenopausal women in the study of Hargreaves and colleagues [11]. The TDLU results for the individual slides (women) comparing areas of high CT density with areas of low CT density are shown in Figure 3. Again, although the results from individual subjects do differ somewhat, the RMRs were not correlated with age (the only variable available on these women) and the summary RMR seems to be a fair representation of the overall results. The results for ducts were again similar. There was no difference in the proliferation rates of epithelial cells in TDLUs and ducts within the same CT density area of individual women (RMR = 1.01, 95% CI 0.98 to 1.04; $p = 0.42$).

More details of the results are provided in the Additional file.

Discussion

Mammographic density is a very strong risk factor for breast cancer. The two groups of investigators [5,6] that studied random biopsies (single slides) from women with different mammographic densities found that the extent of mammographic densities was most strongly correlated with the amount of collagen on the slide. A weaker correlation was found with the amount of epithelial tissue. The findings reported here suggest that the relation between the extent of mammographic density and the amount of epithelial tissue is directly related to the increased concentration of collagen (the main component of

'connective tissue' as shown by collagen staining; see Figure 1) in women with high mammographic densities, because breast epithelium is overwhelmingly confined to areas of high CT density. In the earlier studies of random biopsies [5,6] the weaker relationship between mammographic density and epithelium concentration than between mammographic density and collagen concentration could be simply due to the much greater statistical variability of epithelial tissue in a random slide than one would see for collagen, which occupies a much greater extent of the slide. These results suggest that the increasing breast cancer risk associated with increasing mammographic density might be simply a reflection of more breast epithelial tissue.

We found that the proliferation rate of epithelial cells in areas of high CT density was much lower than in areas of low CT density, arguing against the possibility that dense stroma has a growth factor role in the increased breast cancer risk of women with mammographically dense breasts. In the study of Stomper and colleagues [8], comparison was made between single biopsies of either fat or dense areas in different women; they found no difference in the proliferation rates in the dense and fat areas. Further work is warranted but there is clearly no evidence that areas of high CT density are associated with increased proliferation.

Our results were obtained by conducting a comprehensive count of all the cells in each slide per subject (instead of counting a selected region) and allowed the comparison of proliferation rates in areas of differing CT density within an individual. This permitted us to control completely automatically for factors such as age, menopausal status, or time in the menstrual cycle in the analysis. This gave us great statistical power so that highly statistically significant results could be obtained even with small numbers of subjects.

This study used tissue obtained at reduction mammoplasty performed on women with large breasts. We do not believe that this affects the validity of our findings because the tissue samples were taken deep in the breast away from the subcutaneous fat, but this requires confirmation in future studies. Further studies are also needed relating the CT densities to such risk factors as parity and to understand the biology of the relationship between CT densities and breast epithelium.

Conclusion

The basis of the strong relationship between mammographic density and breast cancer risk may be simply that mammographically dense breasts contain more breast epithelial tissue. Why breast epithelial tissue should be associated with CT densities is not known. Does breast epithelium induce densities? Alternatively, can breast epithelium effectively survive only in areas of densities? Understanding the nature of the interaction between dense CT stroma and epithelial tissue should be a major focus of breast cancer research.

Competing interests

The authors declare that they have no competing interests.

Authors' contributions

DH, AHW, CLP and MCP participated in the design of the study. DH supervised the preparation of the slides and analyzed the slides with the ACIS II system. SD performed all the reduction mammoplasties that provided the tissues used in this analysis and consulted on the tissue obtained from reduction mammoplasties. SB consulted on the interpretation of the results and provided insight into the relationship between mammographic densities and tissue characteristics. CLP coordinated the study. MCP supervised the statistical analysis which was carried out by PW. AHW, CLP and MCP conceived of the study. MCP, DH and AHW drafted the manuscript; all authors read and approved the final manuscript.

Additional files

The following Additional files are available online:

Additional File 1

A Word file containing two tables of detailed results from this study.
See http://www.biomedcentral.com/content/supplementary/bcr1408-S1.doc

Acknowledgements

This work was supported by a Department of Defense Congressionally Mandated Breast Cancer Program Grant BC 044808, by the USC/Norris Comprehensive Cancer Center Core Grant P30 CA14089, and by generously donated funds from the endowment established by Flora L Thornton for the Chair of Preventive Medicine at the USC/Norris Comprehensive Cancer Center. The funding sources had no role in this report.

References

1. Saftlas AF, Szklo M: **Mammographic parenchymal patterns and breast cancer risk.** *Epidemiol Rev* 1987, **9:**146-174.
2. Boyd NF, Lockwood GA, Byng JW, Tritchler DL, Yaffe MJ: **Mammographic densities and breast cancer risk.** *Cancer Epidemiol Biomarkers Prev* 1998, **7:**1133-1144.
3. Ursin G, Hovanessian-Larsen L, Parisky YR, Pike MC, Wu AH: **Greatly increased occurrence of breast cancers in areas of mammographically dense tissue.** *Breast Cancer Res* 2005, **7:**R605-R608.
4. Perkins CI, Hotes J, Kohler BA, Howe HL: **Association between breast cancer laterality and tumor location, United States, 1994-1998.** *Cancer Causes Control* 2004, **15:**637-645.
5. Alowami S, Troup S, Al-Haddad S, Kirkpatrick I, Watson PH: **Mammographic density is related to stroma and stromal proteoglycan expression.** *Breast Cancer Res* 2003, **5:**R129-R135.
6. Li T, Sun L, Miller N, Nicklee T, Woo J, Hulse-Smith L, Tsao M-S, Khokha L, Martin L, Boyd N: **The association of measured breast tissue characteristics with mammographic density and other risk factors for breast cancer.** *Cancer Epidemiol Biomarkers Prev* 2005, **14:**343-349.
7. Bartow SA, Pathak DR, Black WC, Key CR, Teaf SR: **The prevalence of benign, atypical and malignant breast lesions in pop-**

ulations at different risk for breast cancer. *Cancer* 1987, **60:**2751-2760.
8. Stomper PC, Penetrante RB, Edge SB, Arredondo MA, Blumenson LE, Stewart CC: **Cellular proliferative activity of mammographic normal dense and fatty tissue determined by DNA S phase percentage.** *Breast Cancer Res Treat* 1996, **37:**229-236.
9. Shi S-R, Cote R, Chaiwun B, Young LL, Shi Y, Hawes D, Chen T, Taylor CR: **Standardization of immunochemistry based on antigen retrieval technique for routine formalin-fixed tissue sections.** *Appl Immunohistochem* 1998, **6:**89-96.
10. Bartow SA, Mettler FA, Black WC, Moskowitz M: **Correlations between radiographic patterns and morphology of the female breast.** *Prog Surg Path* 1982, **4:**263-275.
11. Hargreaves DF, Potten CS, Harding C, Shaw LE, Morton MS, Roberts SA, Howell A, Bundred NJ: **Two-week dietary soy supplementation has an estrogenic effect on normal premenopausal breast.** *J Clin Endocrinol Metab* 1999, **84:**4017-4024.

Progesterone and Estrogen Receptors in Pregnant and Premenopausal Non-Pregnant Normal Human Breast

DeShawn Taylor* • Celeste Leigh Pearce* • Linda Hovanessian-Larsen* • Susan Downey* • Darcy V. Spicer • Sue Bartow • Chen Ling • Malcolm C Pike • Anna H Wu • and Debra Hawes

*These authors are to be considered joint first authors of this report based on their pivotal contributions to the studies reported here.

D. Taylor
Department of Obstetrics and Gynecology, LAC/USC Women's and Children's Hospital,
Los Angeles, CA. 90033

C.L. Pearce • C. Ling • M.C. Pike • A.H. Wu
Department of Preventive Medicine, Keck School of Medicine, University of Southern California,
Los Angeles, CA. 90033

L. Hovanessian-Larsen
Department of Radiology, Keck School of Medicine, University of Southern California,
Los Angeles, CA. 90033

S. Downey
Department of Surgery, Keck School of Medicine, University of Southern California,
Los Angeles, CA. 90033

D.V. Spicer
Department of Medicine, Keck School of Medicine, University of Southern California,
Los Angeles, CA. 90033

S. Bartow
Department of Pathology, University of New Mexico,
Albuquerque, New Mexico 87131

D. Hawes
Department of Pathology, Keck School of Medicine, University of Southern California,
Los Angeles, CA. 90033

Corresponding author and reprint requests to: Dr. M. C. Pike, USC/Norris Comprehensive Cancer Center, 1441 Eastlake Avenue, Los Angeles, CA 90033; Tel: 323-865-0405; Fax: 323-865-0125; E-mail: mcpike@usc.edu

Abstract
We report here our studies of progesterone and estrogen receptors (PRA, PRB, ERα) in the terminal duct lobular unit (TDLU) epithelium of 21 naturally cycling premenopausal women undergoing reduction mammoplasty and 30 pregnant women. PRA, PRB and ERα were all nuclear except in pregnant subjects who also had extensive cytoplasmic PRB and ERα. PRA expression decreased from a mean of 25.5% in cycling subjects to 4.9% in pregnant subjects, PRB increased from 50.7% to 62.0% (nuclear) and 94.8% (total), ERα increased from 9.2% to 13.0% (nuclear) and 47.0% (total), and epithelial-cell proliferation (MIB1) increased from 2.9% to 18.0%. Decreased PRA expression may endure for a few years after delivery. MIB1 expression was lower in parous women (1.0% vs 3.8%), there was also evidence of a decrease with parity in ERα (7.3% vs 10.2%) and in PRA (18.6% vs 28.9%), but the results were not statistically significant. There are some similarities between these findings and the findings in the rat, but there are also marked differences. Short term changes in PRA expression may be a marker of the effect of pregnancy on the breast which could be used to monitor the effect of chemoprevention regimens aimed at mimicking the effect of pregnancy on the breast.

Keywords Breast • Estrogen Receptor • Progesterone Receptor • Parity • Pregnancy

Introduction

The progesterone receptor (PR) is expressed in two isoforms, progesterone receptor A (PRA) and progesterone receptor B (PRB). Kariagina and colleagues (1) described the varying expression of these two receptors in the breast epithelium of nulliparous and parous rats at differing ages, and noted that the results differed radically from the results seen in mice (2). Their major findings in rats were: (i) The percentage of lobular cells expressing PRA (PRA+ cells) declined steadily from 6 weeks of age (puberty) to 14 weeks of age in nulliparous rats, was much lower during pregnancy (8-10 d of pregnancy) and only partly recovered after involution. (ii) The percentage of PRB+ lobular cells was relatively constant from 3 to 14 weeks of age in nulliparous rats, and was not altered during pregnancy or after involution. These authors suggested that, since human and rat mammary glands share many features (3, 4), their finding might be applicable to the human breast. These findings in rats suggested that measuring PRA may be a simple method of distinguishing a parous from a nulliparous breast, which, if substantiated in the human breast, may be most helpful as a relatively easily obtained biomarker of success in chemoprevention efforts aimed at achieving the protection associated with an early pregnancy.

There are few data available on PRA and PRB expression in normal human breast tissue. We report here our findings regarding PRA and PRB expression in normal human breast tissue obtained from women undergoing reduction mammoplasties as well as from women immediately after a pregnancy termination, *i.e.*, within 10 minutes of the termination. We also report here our findings for estrogen receptor α (ERα) and cell proliferation in these same breast samples.

Materials and Methods

Specimen collection

We retrospectively identified 13 healthy naturally cycling premenopausal women who had undergone a reduction mammoplasty and for whom we could obtain the formalin-fixed paraffin-embedded (FFPE) block of tissue saved from her surgery that had been routinely processed at the University of Southern California Department of Pathology. We also prospectively collected breast tissue (frozen within 30 minutes of excision) from 8 healthy premenopausal women who were undergoing reduction mammoplasty and processed this tissue in a similar manner. These surgeries were all performed by one of us (SD) either at the University of Southern California medical facilities or at the Pacific SurgiCenter.

Ultrasound guided 14-gauge core needle breast biopsy tissue was also prospectively collected from 33 women who had undergone a pregnancy termination within the preceding 10 minutes. Samples of these tissues were processed in a similar manner to that described above, *i.e.*, FFPE in a routine manner at the University of Southern California Department of Pathology. Thirty samples were suitable for analysis.

An in-person interview was conducted with the prospectively recruited mammoplasty subjects and the pregnancy termination subjects, and a telephone interview was conducted with the retrospectively recruited mammoplasty subjects. The interview collected detailed information on reproductive and menstrual factors using a structured questionnaire.

The study protocols were approved by the Institutional Review Board (IRB) of the University of Southern California Keck School of Medicine, and, as appropriate, with the IRBs of St. John's Hospital and Health Center (for Pacific SurgiCenter) and of the Department of Defense Congressionally Directed Breast Cancer Research Program. The prospectively collected samples were obtained after the women had signed an informed consent agreeing to participate in this research. The women from whom the retrospectively collected samples were obtained also provided verbal informed consent agreeing to participate in this research.

Immunohistochemistry

Immunohistochemical (IHC) analysis was performed as follows: For all studies, multiple adjacent FFPE sections were cut at 5 μm, deparaffinized and hydrated. All slides were also subject to antigen retrieval

which was performed by heating the slides in 10 mmol/L sodium citrate buffer (pH 6) at 110°C for 30 minutes in a pressure cooker in a microwave oven (5). Endogenous peroxidase activity was blocked by incubation in 3% H_2O_2 in phosphate-buffered saline for 10 minutes, followed by blocking of nonspecific sites with SuperBlock blocking buffer (Pierce, Rockford, Illinois) for 1 hour both at room temperature (6).

For the single marker studies, the sections were incubated for analysis with the following antibodies: PRA, the mouse monoclonal antibody NCL-PGR-312 (Novocastra Laboratories Ltd., Newcastle upon Tyne, UK) at a concentration of 1:5000; PRB, the mouse monoclonal antibody hPRa6 (Lab Vision, Fremont, California) at a concentration of 1:100; ERα, the mouse monoclonal antibody ER Ab-12 (Clone 6F11) (Neomarkers, Kalamazoo, Michigan) at a concentration of 1:100; and MIB1, a proliferation marker, the mouse monoclonal antihuman Ki67 antigen (Dako Cytomation, Carpenteria, California) at a concentration of 1:500. After incubation with the primary antibodies, antibody binding was localized with the ABC staining kit from Vector Laboratories (Burlingame, California) according to the manufacturer's instructions and peroxidase activity was detected using 3,3'-diaminobenzidine substrate solution (DAB). A wash step with phosphate buffer solutions (PBS) for 10 minutes was carried out between each step of the immunostaining. Slides were counterstained with hematoxylin and mounted in aqueous mounting medium for examination.

A selection of the slides were also double-stained to permit luminal-epithelial and myoepithelial tissue to be clearly distinguished and to evaluate the co-expression of different markers. The myoepithelial cells were detected using an antibody for smooth muscle actin (SMA; Dako Cytomation, Carpenteria, California) at a concentration of 1:800. SMA is localized in the cytoplasm of the cells and is easily distinguished from nuclear staining; on double-stained slides actin was detected using DAB (Biocare, Concord, California). Ferengi blue was the second chromogen for both PRA and PRB. In slides that were double-stained for PRA and PRB, PRA was stained with DAB and PRB with Ferengi Blue (Biocare, Concord, California). No hematoxylin counterstain was applied to the double-stained slides.

In the single-marker slides, we used the Automated Cellular Imaging System II (ACIS II Clarient, Aliso Viejo, California) to assess all terminal duct lobular units (TDLUs) on a single slide or the first 100 target areas containing TDLUs selected systematically from left to right top to bottom on the slide if there were an excessive number of epithelial cells present. A clear distinction between luminal-epithelial cells and myoepithelial cells in TDLUs is frequently difficult to make on conventionally stained slides. For this reason we counted the total numbers of luminal-epithelial + myoepithelial cells (referred to as epithelial cells) and the percentage of them positive for the relevant marker using the ACIS II which is a cellular imaging system that digitizes the images and permits the user to identify and quantitate relevant areas on a high-resolution computer screen based on color differentiation. The ACIS II software program does not function optimally when both nuclear and cytoplasmic staining is present. Due to the high cytoplasmic staining in addition to expected nuclear positivity found in the PRB and ERα slides from the pregnant subjects we used conventional light microscopy and manual counting methods for assessing the TDLUs in these cases. If scant epithelial tissue was present all epithelial cells were counted, in most cases we randomly identified 300 epithelial cells, in cases with an excessively large amount of epithelium present we counted 500 epithelial cells to avoid sampling bias. The percentage of cells positive was determined by identifying the number of cells with nuclear positivity for the selected marker versus those negative or positive.

In the double-marker slides we used the Nuance FLEX™ spectral imaging system (Cambridge Research & Instrumentation, Inc., Woburn, Massachusetts) to assess the co-expression of markers on a single slide.

Statistical analysis

We analyzed this data using standard statistical software (Stata Corporation, Austin, Texas). Differences in expression were tested for significance by the non-parametric Mann-Whitney RankSum test. Non-parametric tests for trend were made using the test devised by Cuzick (7). All statistical significance levels (p values) quoted are two sided.

Results

Non-pregnant subjects

Epithelial staining for PRA, PRB, ERα and MIB1 were all nuclear in non-pregnant subjects. The medians (interquartile ranges) and means (standard errors) of the proportion of epithelial cells with positive nuclear staining for PRA, PRB, ERα and MIB1 in non-pregnant subjects sub-classified by parity (nulliparous vs. parous) are given in Table 1. The individual values for nuclear staining are shown in Fig. 1.

PRA and PRB

A mean of 25.5% and 50.7% of epithelial cells expressed PRA (PRA+ cells) and PRB (PRB+) respectively. There was a higher proportion of cells positive for PRA in nulliparous compared to parous women (mean values: 28.9% vs 18.6%), but this was not statistically significant (p=0.50). There was little difference in the proportion of cells positive for PRB in nulliparous compared to parous women (49.1% vs 53.9%).

PRA was expressed in the luminal epithelium but almost never expressed in the myoepithelium (Fig. 2A). PRB was expressed in the luminal epithelium and in the myoepithelium (Fig. 2B). The proportion of cells expressing PRB in the luminal epithelium appeared to be greater than the proportion expressing PRB in the myoepithelium, but this was difficult to assess completely satisfactorily due to the morphology of the myoepithelial cells which does not permit clear nuclear visualization in many cases.

In the luminal epithelium almost all cells expressing PRA expressed PRB (Fig. 3), but many luminal epithelial cells expressed PRB without expressing PRA.

ERα

A mean of 9.2% of epithelial cells expressed ERα. There was a higher proportion of cells positive for ERα in nulliparous compared to parous women (mean values: 10.2% vs 7.3%), but this was not statistically significant (p=0.66). ERα was not expressed in the myoepithelium.

MIB1

A mean of 2.9% of epithelial cells expressed MIB1. There was a higher proportion of cells positive for MIB1 in nulliparous women compared to parous women (mean values: 3.8% vs 1.0%), but this was again not statistically significant (p=0.23).

MIB1 expression was much lower in the myoepithelium than in the luminal epithelium.

We found no evidence that weight or age affected these results.

Pregnant subjects

The gestational age of the pregnant subjects varied from 5 to 23 weeks (median 8.1 weeks, interquartile range 7.2 to 12.0 weeks). Epithelial staining was nuclear for PRA and MIB1, but PRB and ERα staining was both nuclear and cytoplasmic with cells expressing nuclear alone, nuclear and cytoplasmic, and cytoplasmic alone staining. Results are presented as nuclear staining and total staining (includes nuclear and/or cytoplasmic) in Table 2.

PRA and PRB

A mean of 4.9% of epithelial cells expressed nuclear PRA. A mean of 62.0% of epithelial cells expressed nuclear PRB and total PRB staining was seen in 94.8% of such cells. Fig. 4 shows the sharp difference in PRA and PRB expression.

ERα

A mean of 13.0% of epithelial cells expressed nuclear ERα and total ERα staining was seen in 47.0% of such cells.

MIB1

A mean of 18.0% of epithelial cells expressed nuclear MIB1.

The same cell types expressed these antigens as in the non-pregnant subjects. There was statistically significant evidence (p_{trend}=0.043) of a decline in PRA expression with gestational age; a mean of 6.2% of cells were PRA+ at a gestational age of <12 weeks vs 1.3% at a gestational age of ≥12 weeks (Fig. 5). There was also a statistically significant (p_{trend}= 0.004) decline in nuclear ER expression with gestational age; a mean of 15.5% at a gestational age of <12 weeks vs 5.8% at a gestational age of ≥12 weeks (Fig. 5). Other effects of gestational age were small and not statistically significant.

These results for pregnant women were markedly different from the results in non-pregnant women. PRA expression was much decreased in pregnant women [mean values: 25.5% in non-pregnant subjects vs 4.9% in pregnant subjects (p=0.001)]; PRB was increased [from 50.7% to 62.0% nuclear staining (p=0.11) and 94.8% total staining (p<0.001)]; ERα was increased [from 9.2% to 13.0% nuclear staining (p=0.21) and 47.0% total staining (p<0.001)]; and MIB1 was much increased [2.9% vs 18.0% (p<0.001)].

As can be seen in Fig. 1, the results for PRA, PRB, ERα and MIB1 varied widely between different subjects. The results frequently also varied widely within a single slide; this was due in part to the positive cells tending to cluster within single TDLUs as is illustrated in Fig. 6 for ERα in a non-pregnant subject and as has previously been reported (8).

Expression in fibroblasts

PRA and ERα were virtually never expressed in the non-pregnant or pregnant breast stromal fibroblasts. In contrast, PRB was commonly expressed in fibroblasts (~35% of cells) (Fig. 7) in both non-pregnant and pregnant subjects.

Discussion

Epithelial staining for PRA, PRB, ERα and MIB1 were all nuclear in the non-pregnant subjects as has been previously reported (8-10). The same held for PRA and MIB1 in pregnant subjects, but PRB and ERα were both nuclear and cytoplasmic in pregnant subjects. The differences seen in PRA, PRB, ERα and MIB1 nuclear expression between non-pregnant and pregnant subjects were the most striking results seen here.

PRA expression was decreased from a mean of 25.5% in non-pregnant subjects to 4.9% in pregnant subjects, PRB expression increased from 50.7% to 62.0% (or 94.8% if one includes cytoplasmic staining); ERα expression increased from 9.2% to 13.0% (or 47.0% if one includes cytoplasmic staining), and MIB1 expression from 2.9% to 18.0%. These are the first such results to be reported from a significant number of pregnant subjects. Kariagina *et al.* (1) in their study of Sprague-Dawley rats found a similar, although somewhat lesser, decrease in PRA expression in pregnancy, but they found no difference in PRB expression between non-pregnant and pregnant rats. No ER expression was found in four pregnant subjects in an autopsy study (11); the reason for this is unclear. The increase in breast cell proliferation in early pregnancy is, of course, well known (10).

The results in non-pregnant women were highly variable woman to woman with no statistically significant differences in PRA, PRB or ERα between nulliparous and parous subjects. However, PRA was 36% lower in parous subjects, a result similar to that seen in the rat (1), where PRA expression was significantly lower in parous (4 weeks after weaning) rats compared to “age-matched” (1) virgin controls (20% vs 11%). The larger difference seen in rats could be due to the recency of the pregnancy as the results in rats were from rats only 4 weeks post lactation. In the study reported here, the three parous non-pregnant subjects whose last pregnancy was within five years of their surgery had very low (0.5%, 2.7%

and 3.8%) PRA expression. We are currently obtaining follow-up samples from the pregnant subjects to evaluate this further.

Expression of PRB in non-pregnant women was much more frequent in the breast TDLU epithelial cells (50.7%) than was the expression of PRA (25.5%). This was, in part, due to the fact that PRB was frequently expressed in myoepithelial cells as well as in luminal epithelial cells (Fig. 2), whereas PRA expression was almost exclusively confined to luminal epithelial cells. This effective restriction of PRA to luminal cells, while PRB was expressed in both types of epithelium, was also found in the rat (1). These results are, however, in conflict with the results reported by Mote *et al.* that PRA and PRB were "co-expressed at similar levels" (12). Their study was performed on FFPE breast tissue samples from autopsies of premenopausal women obtained some 20 years previously by one of us (13). We were unsuccessful at staining these autopsy specimens for PRA or PRB. Further independent study of this question is needed.

In the rat, Kariagina *et al.* (1) found that PRB was more frequently expressed in myoepithelial cells than in luminal cells (~95% vs ~60% for all epithelial cells). We did not see this. The proportion of cells expressing PRB in the luminal epithelium appeared to be greater than the proportion expressing it in the myoepithelium; however, this was difficult to assess completely satisfactorily due to the morphology of the myoepithelial cells which did not permit clear nuclear visualization in many cases.

Our finding that PRB expression was common in stromal fibroblasts (Fig. 6) fits in well with the study of Humphreys and colleagues (14) in the mouse which found that stromal PRB expression was essential for ductal development. PR was not found in fibroblasts in an earlier study (15) but it is unclear if the antibody used would have detected PRB. However, Mote *et al.* (16) also reported no staining of stromal cells in their study of "morphologically normal breast tissue taken from benign breast biopsy specimens" using the same antibody we used. Further independent study of this question is also needed.

Although estrogen receptor β, ERβ, is present in a high proportion of luminal and myoepithelial cells in the normal human breast, knock-out studies have shown that ERα is the key ER in the breast (17, 18). ERα is found in the luminal epithelium but not in any other cell type in the breast (6, 19). Although it is sometimes stated that all cells expressing PR also express ERα (19), this is, of course, not true in the human breast as evidenced by the fact that PR is much more frequently expressed than ERα (17, 20). We found some evidence of a decrease in ERα expression in parous women.

A reduction in breast cell proliferation and of ERα may be useful markers of the reduction in risk with pregnancy. However, the extent of the overlap (Fig. 1) between the results from nulliparous and parous women mean that large numbers of subjects will be required if they are to be used to establish such an effect with any chemoprevention regimen aimed at mimicking pregnancy. Short-term changes in PRA expression may be a more useful marker.

Acknowledgements

We wish to express our sincerest gratitude to the women who agreed to be part of these studies. We also wish to express our thanks to Ms. Peggy Wan and Ms. A. Rebecca Anderson for extensive help with the management of the study and the statistical analysis. This work was supported by a Department of Defense Congressionally Directed Breast Cancer Research Program Grant BC 044808, by the USC/Norris Comprehensive Cancer Center Core Grant P30 CA14089, funds from the endowment established by Flora L. Thornton for the Chair of Preventive Medicine at the Keck School of Medicine of USC and an anonymous donor grant to DT. The funding sources had no role in this report.

Disclosure statement: The authors declare that they have nothing to disclose.

References

1. Kariagina A, Aupperlee MD, Haslam, SZ (2007) Progesterone receptor isoforms and proliferation in the rat mammary gland during development. Endocrinology 148:2723-2736
2. Aupperlee MD, Smith KT, Kariagina A, Haslam SZ (2005) Progesterone receptor isoforms A and B: temporal and spatial differences in expression during murine mammary gland development. Endocrinology 146:3577-3588
3. Russo J, Russo IH (1996) Experimentally induced mammary tumors in rats. Breast Cancer Res Treat 39:7-20
4. Russo IH, Russo J (1998) Role of hormones in mammary cancer initiation and progression. J Mammary Gland Biol Neoplasia 3:49-61
5. Taylor CR, Shi SR, Chen C, Young L, Yang C, Cote RJ (1996) Comparative study of antigen retrieval heating methods: microwave, microwave and pressure cooker, autoclave, and steamer. Biotech Histochem 71:263-270
6. Cuzick J (1985) Wilcoxon-type test for trend. Statist Medicine 4:87-89
7. Kumar SR, Singh J, Xia G, Krasnoperov V, Hassanieh L, Ley EJ, Scehnet J, Kumar NG, Hawes D, Press MF et al (2006) Receptor tyrosine kinase EphB4 is a survival factor in breast cancer. Am J Pathol 169:279-293
8. Shoker BS, Jarvis C, Sibson DR, Walker C, Sloane JP (1999) Oestrogen receptor expression in the normal and pre-cancerous breast. J Pathol 188:237-244
9. Petersen OW, Hoyer PE, van Deurs B (1987) Frequency and distribution of estrogen receptor-positive cells in normal, nonlactating human breast tissue. Cancer Res 47:5748-5751
10. Suzuki R, Atherton AJ, O'Hare MJ, Entwistle A, Lakhani SR, Clarke C (2000) Proliferation and differentiation in the human breast during pregnancy. Differentiation 66:106-115
11. Bartow SA (1998) Use of the autopsy to study ontogeny and expression of the estrogen receptor gene in human breast. J Mammary Gland Biol Neoplasia 3:37-48
12. Mote PA, Bartow S, Tran N, Clarke CL (2002) Loss of co-ordinate expression of progesterone receptors A and B is an early event in breast carcinogenesis. Breast Cancer Res Treat 72:163-172
13. Longacre TA, Bartow SA (1986) A correlative morphologic study of human breast and endometrium in the menstrual cycle. Am J Surg Pathol 10:382-393
14. Humphreys RC, Lydon J, O'Malley BW, Rosen JM (1997) Mammary gland development is mediated by both stromal and epithelial progesterone receptors. Mol Endocrinol, 11:801-811
15. Russo J, Ao X, Grill C, Russo IH (1999) Pattern of distribution of cells positive for estrogen receptor alpha and progesterone receptor in relation to proliferating cells in the mammary gland. Breast Cancer Res Treat 53:217-227
16. Mote PA, Leary JA, Avery KA, Sandelin K, Chenevix-Trench G, kConfab Investigators, Kirk JA, Clarke CL (2004) Germ-line mutations in BRCA1 or BRCA2 in the normal breast are associated with altered expression of estrogen-responsive proteins and the predominance of progesterone receptor A. Genes Chromos Cancer 39:236-248
17. Speirs V, Skliris GP, Burdall SE, Carder PJ (2002) Distinct expression patterns of ER alpha and ER beta in normal human mammary gland. J Clin Pathol 55:371-374
18. Couse JF, Korach KS (1999) Estrogen receptor null mice: what have we learned and where will they lead us? Endocr Rev 20:358-417
19. Clarke RB, Howell A, Potten CS, Anderson E (1997) Dissociation between steroid receptor expression and cell proliferation in the human breast. Cancer Res 57:4987-4991
20. Soderqvist G, von Schoultz B, Tani E, Skoog L (1993) Estrogen and progesterone receptor content in breast epithelial cells from healthy women during the menstrual cycle. Am J Obstet Gynecol 168:874-879

TABLE 1. Median (interquartile range) and mean (standard error) percentages of PRA, PRB, ERα and MIB1 nuclear staining in premenopausal non-pregnant nulliparous and parous subjects

	Nulliparous	Parous	Total
N	14	7	21
PRA	27.1 (5.9-39.6)	16.5 (2.7-33.6)	21.2 (3.8-38.8)
	28.9 (6.9)	18.6 (6.5)	25.5 (5.1)
PRB	52.9 (32.2-61.3)	59.8 (27.2-78.9)	54.0 (32.2-70.1)
	49.1 (6.8)	53.9 (9.9)	50.7 (5.5)
ERα	12.0 (2.8-14.0)	4.5 (3.0-14.5)	8.0 (2.9-14.2)
	10.2 (2.2)	7.3 (2.7)	9.2 (1.7)
MIB1	1.6 (0.7-4.3)	1.0 (0.4-1.4)	1.0 (0.5-2.3)
	3.8 (1.3)	1.0 (0.3)	2.9 (0.9)

TABLE 2. Median (interquartile range) and mean (standard error) percentages of PRA, PRB, ERα and MIB1 nuclear and total staining in pregnant and premenopausal non-pregnant subjects

	Pregnant		Non-Pregnant
	Nuclear Only	Nuclear and/or Cytoplasmic	Nuclear Only
N	30	30	21
PRA	3.6 (1.0-8.2) 4.9 (0.8)	–	21.2 (3.8-38.8) 25.5 (5.1)
PRB	70.0 (42.0-78.5) 62.0 (4.8)	96.5 (93.1-97.5) 94.8 (0.8)	54.0 (32.2-70.1) 50.7 (5.5)
ERα	12.0 (3.7-18.0) 13.0 (1.8)	41.0 (17.9-71.8) 47.0 (5.3)	8.0 (2.9-14.2) 9.2 (1.7)
MIB1	16.5 (11.5-23.5) 18.0 (1.8)	–	1.0 (0.5-2.3) 2.9 (0.9)

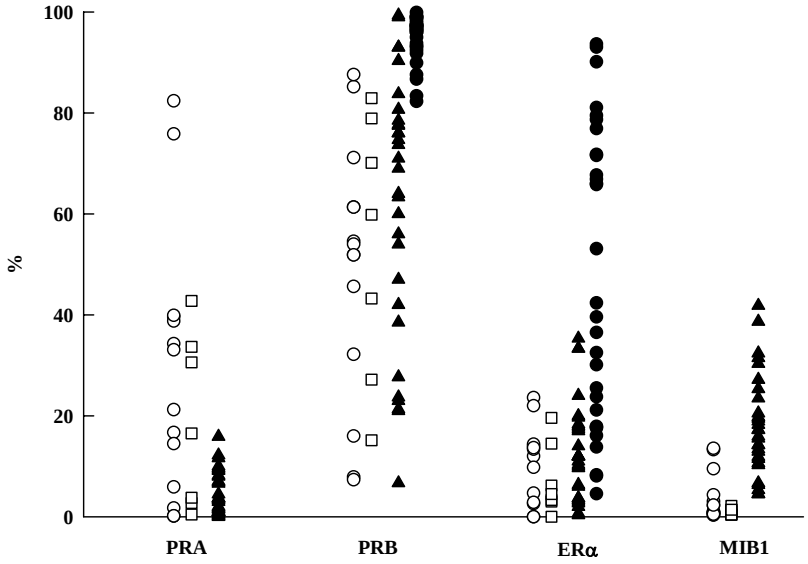

FIG. 1. % of cells expressing nuclear PRA, nuclear and total PRB and ERα and nuclear MIB1 in premenopausal nulliparous (○), premenopausal parous (□) and pregnant (nuclear(▲) and total (●)) women.

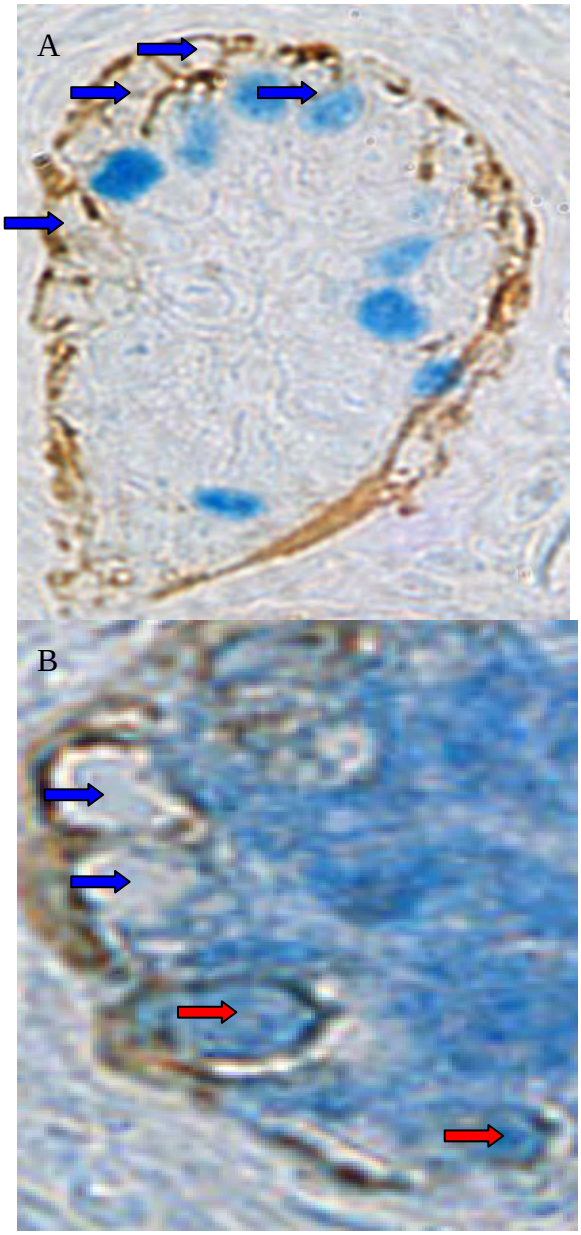

FIG. 2. Double staining for PRA (blue) and SMA (brown) showing myoepithelial cells are negative for PRA (blue arrows) (A). Double staining for PRB (blue) and SMA (brown) showing myoepithelial cells positive (red arrows) and negative (blue arrows) for PRB (B).

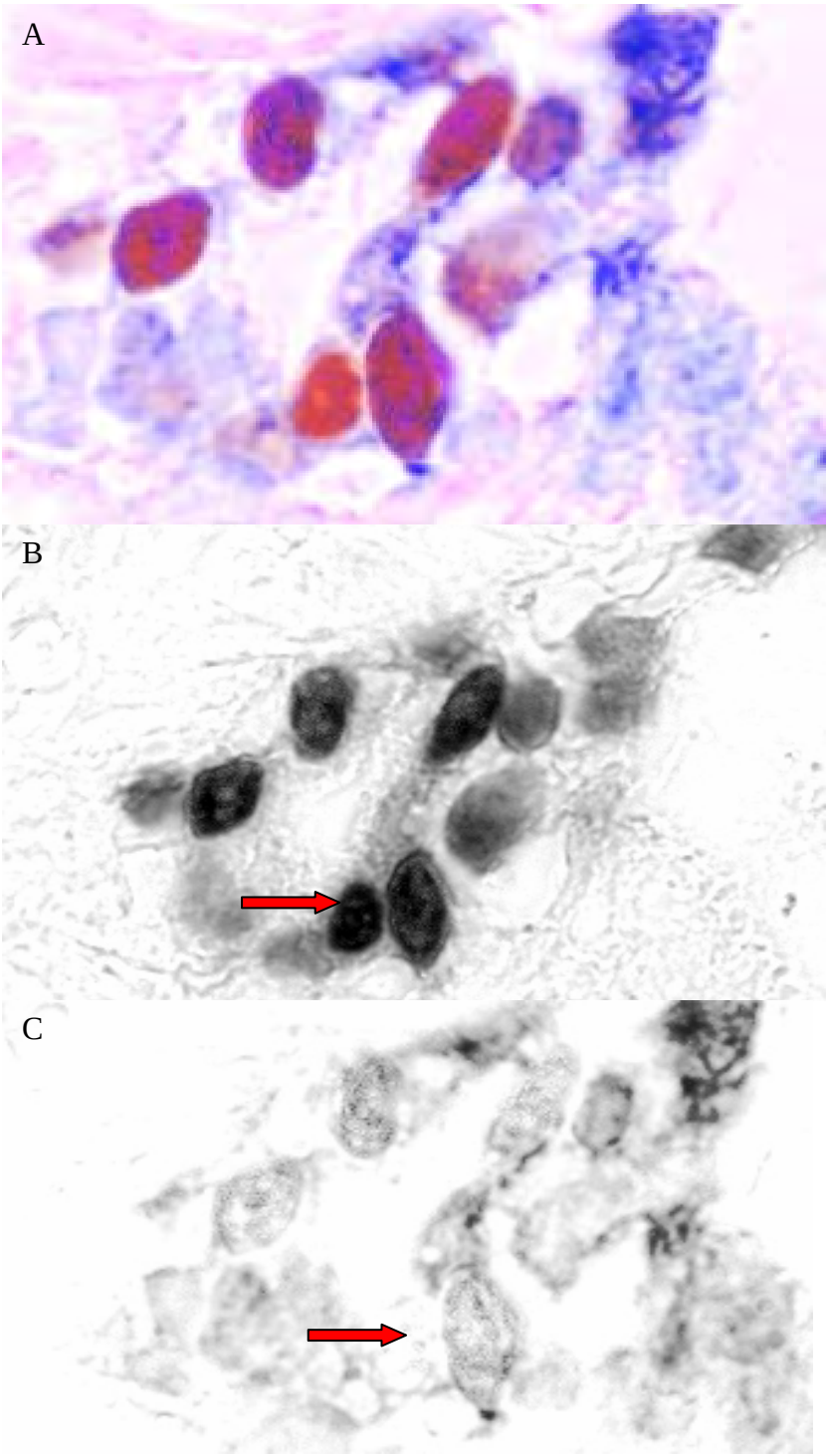

FIG. 3. Composite spectral image showing PRA (red) and PRB (blue) positive cells (A). PRA positive cells only are shown in B. C shows PRB positive cells only and that all but one (red arrow) PRA positive cells coexpress PRB.

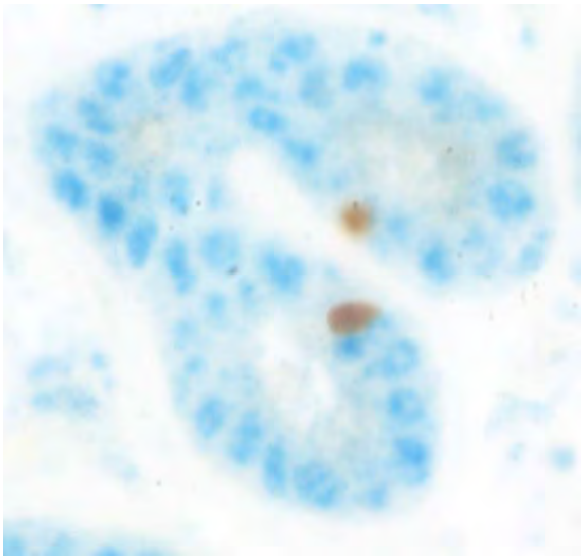

FIG. 4 . Double-stained slide showing a preponderance of PRB (blue) positive cells and few PRA (brown) cells in a pregnant subject.

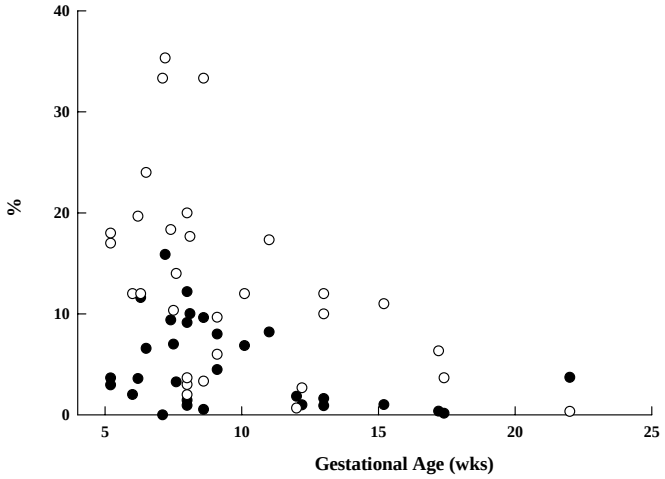

FIG. 5. Nuclear PRA (●) and ERα (○) expression in pregnant women by gestational age.

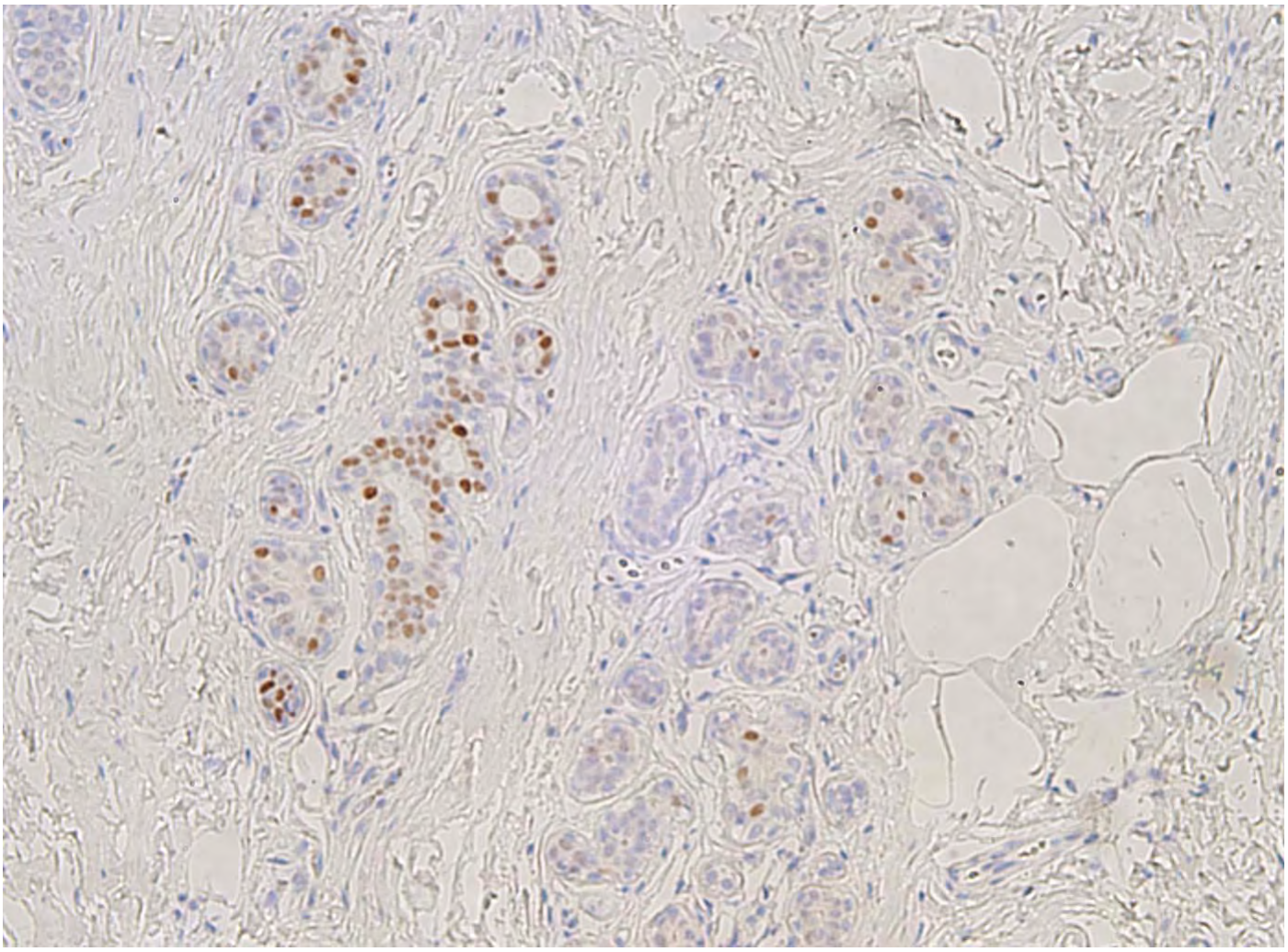

FIG. 6. Number of ER positive cells (brown nuclei) can vary significantly between TDLUs as seen in this photomicrograph .

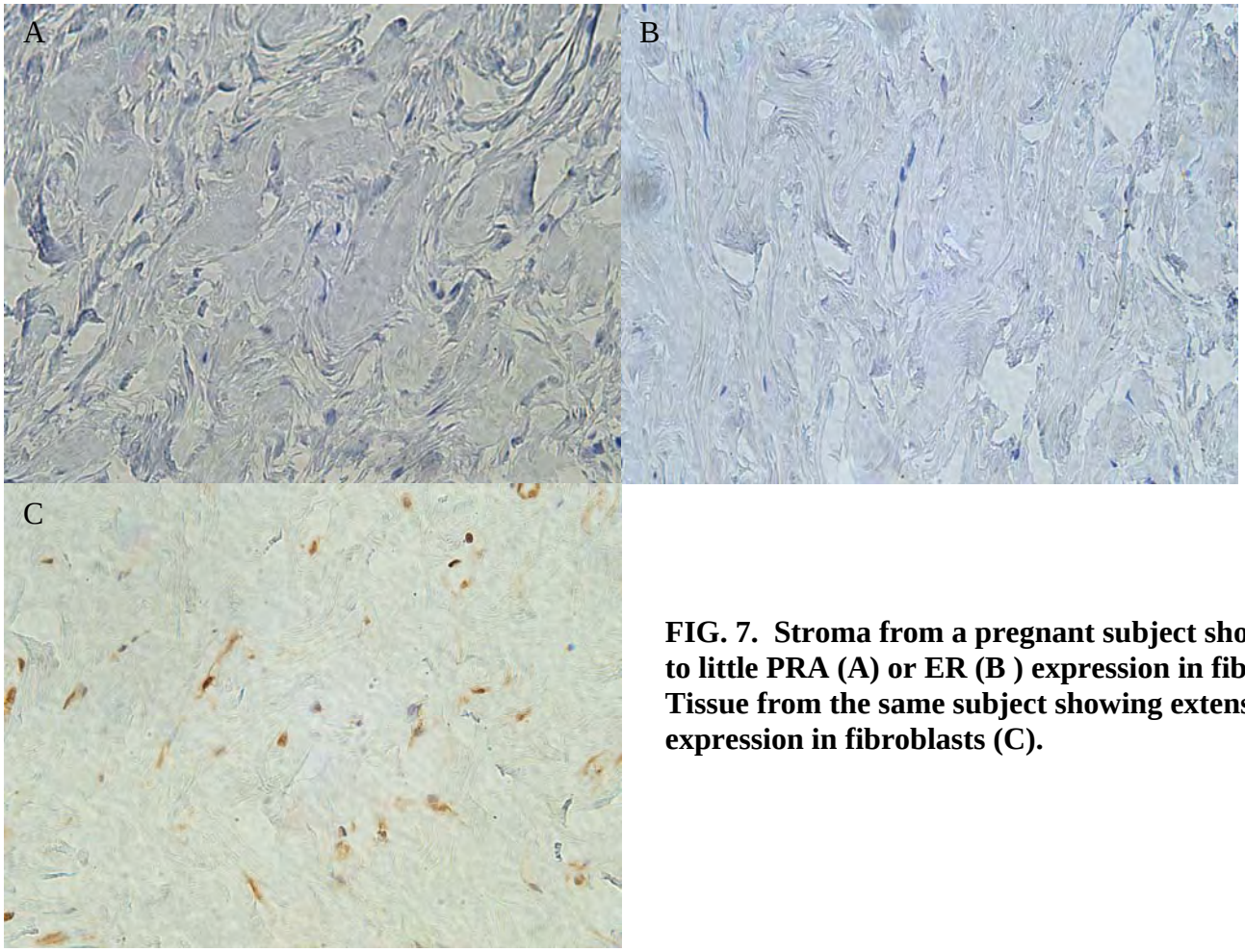

FIG. 7. Stroma from a pregnant subject showing no to little PRA (A) or ER (B) expression in fibroblasts. Tissue from the same subject showing extensive PRB expression in fibroblasts (C).